



Effects of removal of the axial methionine heme ligand on the binding of *S. cerevisiae* iso-1 cytochrome *c* to cardiolipin

Alessandro Paradisi^b, Marzia Bellei^b, Carlo Augusto Bortolotti^b, Giulia Di Rocco^b, Antonio Ranieri^b, Marco Borsari^a, Marco Sola^b, Gianantonio Battistuzzi^{a,*}

^a Department of Chemistry and Geology, University of Modena and Reggio Emilia, via Campi 103, 41126 Modena, Italy

^b Department of Life Sciences, University of Modena and Reggio Emilia, via Campi 103, 41126 Modena, Italy

ARTICLE INFO

Keywords:

Cytochrome *c*
Cardiolipin
Heme axial ligation
Electronic absorption spectroscopy
MCD
Fluorescence emission spectroscopy

ABSTRACT

The cleavage of the axial S(Met) – Fe bond in cytochrome *c* (cyt*c*) upon binding to cardiolipin (CL), a glycerophospholipid of the inner mitochondrial membrane, is one of the key molecular changes that impart cyt*c* with (lipo)peroxidase activity essential to its pro-apoptotic function. In this work, UV – VIS, CD, MCD and fluorescence spectroscopies were used to address the role of the Fe – M80 bond in controlling the cyt*c*-CL interaction, by studying the binding of the Met80Ala (M80A) variant of *S. cerevisiae* iso-1 cyt*c* (ycc) to CL liposomes in comparison with the wt protein [Paradisi et al. J. Biol. Inorg. Chem. 25 (2020) 467–487]. The results show that the integrity of the six-coordinate heme center along with the distal heme site containing the Met80 ligand is a not requisite for cyt*c* binding to CL. Indeed, deletion of the Fe – S(Met80) bond has a little impact on the mechanism of ycc-CL interaction, although it results in an increased heme accessibility to solvent and a reduced structural stability of the protein. In particular, M80A features a slightly tighter binding to CL at low CL/cyt*c* ratios compared to wt ycc, possibly due to the lift of some constraints to the insertion of the CL acyl chains into the protein hydrophobic core. M80A binding to CL maintains the dependence on the CL-to-cyt*c* mixing scheme displayed by the wt species.

1. Introduction

Eukaryotic cytochrome *c* (cyt*c*) is a small globular protein located in the periplasmic space of mitochondria [1–9]. Its six-coordinate heme *c* forms two thioether bonds with the sidechains of Cys15 and Cys17 and is surrounded by a hydrophobic environment, whereas its proximal and distal axial coordination positions are occupied by a histidine (His18) and a methionine (Met80), respectively [1–7,9,10]. Due to its stability, availability and peculiar spectroscopic and redox properties, cytochrome *c* has been widely used as a model system to unravel the molecular details of biological electron transfer [1,11–16] and protein folding [5,17–25].

Mitochondrial cyt*c* is best known as an electron transfer protein, shuttling electrons from complex III of the mitochondrial respiratory chain to cytochrome *c* oxidase [1–3,6,9]. However, it is also an effective antioxidant and detoxifying agent, scavenging reactive oxygen species (ROS) from healthy cells [8,26]. Moreover, upon ejection out of the mitochondrion, cytochrome *c* exerts an important pro-apoptotic

function by forming a multimeric complex with Apaf-1, ATP and procaspase-9 (apoptosome) [1,4,5,8,27–31]. The latter function is related to its specific interaction with cardiolipin (CL), a negatively charged glycerophospholipid forming the 25% of the total lipid content of the inner mitochondrial membrane (IMM) [8,27–30,32,33]. This interaction results in a strong binding of the protein to the IMM [34–37], which induces its unfolding and the cleavage of the Fe – S(Met80) bond, imparting cyt*c* with a significant (lipo)peroxidase activity, essential to its pro-apoptotic function [1,5,8,9,27,29,30,33,38–43].

Understanding of the molecular details controlling the cyt*c*-CL interaction is crucial to unravel the molecular origin of partition of the protein between its respiratory, antioxidant and proapoptotic functions [1,5,36,37,42,44,45]. Extensive research [1,5,20,27,28,36,37,41,42,44,46–63] has revealed the existence of multiple protein-CL interaction modes, which turn out to be sensibly influenced by the experimental conditions (pH, ionic strength, CL liposome type and content, protein coverage and curvature of the membrane surface), affecting both the distribution of the protein structures and the degree of CL-induced protein

* Corresponding author.

E-mail address: gianantonio.battistuzzi@unimore.it (G. Battistuzzi).

<https://doi.org/10.1016/j.jinorgbio.2023.112455>

Received 23 September 2023; Received in revised form 5 December 2023; Accepted 13 December 2023

Available online 18 December 2023

0162-0134/© 2023 The Author(s). Published by Elsevier Inc. This is an open access article under the CC BY license (<http://creativecommons.org/licenses/by/4.0/>).

unfolding [1,5,28,36,37,39,41,42,44,46,47,64–66]. In spite of their heterogeneity, the data available demonstrate that cytc binding to CL-containing membranes is guided by electrostatic forces as well as by hydrophobic interactions [1,5,28,33,35–37,42–44,47,50,51,64,65,67–69].

Due to the above-mentioned data heterogeneity, it is not surprising that different mechanisms have been proposed for cytc anchoring to CL membranes. The “extended lipid anchorage” hypothesis [1,8,29,30,34,35,37,49,57,69–75] assumes that after electrostatic interaction with a cluster of surface lysines, one or two CL acyl chains insert into cytc hydrophobic core forcing the protein into a more open conformation and disrupting the Fe – S(Met80) bond. Alternatively, a “peripheral binding mechanism” was proposed [41,45,46,62,65,67,76,77] according to which CL-bound cytc exists in a globular, non-native form (C form) in equilibrium with a largely unfolded species (E form), responsible of the observed lipoperoxidase activity [41,45,46,62,65,67,76,77]. Cyt crowding on the membrane surface significantly influences the relative amount of the two species, as the equilibrium progressively shifts from the C to the E form as the membrane surface becomes less crowded [45,51,65,78,79]. Moreover, it appears that the concave curvature of the IMM may significantly influence the conformational rearrangements of cytc as well as its peroxidase activity in the early stages of apoptosis, since its behavior changes upon binding to concave or convex membrane surfaces [65]. Recently, it was suggested that the extended lipid anchorage mechanism and the peripheral binding mechanism prevail at low and high CL/cytochrome *c* molar ratios, respectively [39].

The disruption of the Fe – M80 bond upon interaction of ferric cytc with CL-containing vesicles leads to a main low-spin six-coordinate His/His species in equilibrium with a limited amount of a high-spin five-coordinate species, featuring a Fe-His metal center [1,5,8,15,30,34,36,37,39,45,49,53,54,59,75,80–82]. This change in axial coordination is required to turn CL-bound cytochrome *c* into an efficient lipoperoxidase able to catalyze the peroxidation of CL. Consistently, the Met80Ala (M80A) variant of cytochrome *c* (lacking the Fe – M80 bond) and the bis-His axially-ligated cytc conformers possess increased peroxidase and nitrite reductase activities and can mediate the electrocatalytic reduction of O₂ [15,24,81,83–90]. Interestingly, the spontaneous release of M80A from mitochondria to the cytoplasm and nucleus does not induce apoptosis, possibly as a result of its inability to activate the apoptosome [84]. Beyond CL interaction, disruption of Fe – M80 ligation and axial ligand swapping were observed also upon tyrosine nitration under nitrate stress conditions [1,37,53,63,84,91–94] and cytc adsorption onto structured molecular assemblies [89,95].

Surprisingly, the role of the Fe – M80 bond in controlling the cytc-CL interaction has not been specifically addressed so far. To clarify this issue, in this work we analyzed the binding of the M80A variant of *S. cerevisiae* iso-1 cytochrome *c* (ycc hereafter) [15,24,25,83,85–87,96–101] to CL liposomes [35,53,64,73,74,80,102] in comparison with that of the wt protein using different spectroscopic techniques (UV – vis, CD, MCD and fluorescence emission). Since the mechanism of cytc binding to anionic CL liposomes is significantly influenced by CL/protein ratio [1,5,8,30,37,39,42,44–46,65,79], the study was carried out both at low (from 0.5 to 10) and high (from 5 to 60) CL/M80A molar ratios, using the same experimental conditions previously applied for wt ycc and its KtoA mutants [39]. We found that M80A does specifically bind to CL-containing membranes and that the structural and stability effects induced by the deletion of the Fe-M80 bond has a limited impact on the mechanism of the cytc-CL interaction, which in turn confirms its marked dependence on the way CL and cytc are added. Moreover, the increased heme accessibility of M80A to solvent results in an enhanced affinity for CL at low CL/cytc molar ratios compared to wt ycc, possibly due to the easier insertion of the CL acyl chains into the protein hydrophobic core.

2. Experimental

2.1. Materials

CL from bovine heart (3.92 mM ethanolic solution, purity ≥97%) was purchased from Sigma Chemical Co. and used without further purification. All chemicals were reagent grade. Doubly distilled water was used throughout.

2.2. Protein production and isolation

The M80A mutant of recombinant *S. cerevisiae* iso-1 cytochrome *c* (M80A hereafter) was expressed and isolated as described previously [85–87,99,103]. The variant is nontrimethylated and carries the C102T mutation to prevent protein dimerization [85–87,99,103].

2.3. Spectroscopic measurements

The interaction between M80A and CL was investigated following the changes induced in the electronic absorption (360–460 nm), CD (240–320 nm and 360–460 nm) and MCD (360–460 nm) spectra as well as in the fluorescence emission spectra (308–560 nm) of the protein by stepwise addition of a few microliters of a 3.9 mM CL ethanolic solution to protein buffered solutions [35,39,53,64,73,74,80,102]. All experiments were carried out at 25 °C with protein solutions freshly prepared before use in 5 mM HEPES buffer at pH 7; the protein concentration was checked spectrophotometrically, using $\epsilon_{405} = 121,700 \text{ M}^{-1} \text{ cm}^{-1}$ [96,97]. Initial protein concentration was 5 μM . The electronic absorption, CD and MCD spectra were recorded with a Jasco J-810 spectropolarimeter using a quartz cuvette of 0.5 cm path length. In all cases, spectra were recorded 20 min after mixing. As no further spectroscopic changes were observed for longer waiting times, we assumed that equilibrium conditions were achieved 20 min after mixing. The magnetic field for MCD measurements was provided by a GMW Magnet system Model 3470 split coil superconductivity magnet with a maximum field of 1 Tesla (T). Both CD and MCD spectra were measured in $\theta = \text{mdeg}$. The former were converted to molar ellipticity $[\theta]$ using the conversion factor $[\theta] = \theta(\text{deg}) \bullet 100/(d \bullet c)$, where *c* is the protein concentration (mol/dm³) and *d* is the thickness of the sample (path length, 0.5 cm) [22,104,105], while the latter were converted to $\Delta\epsilon$ [$\text{M}^{-1} \text{ cm}^{-1} \text{ T}^{-1}$] using the conversion factor $\Delta\epsilon = \theta/(32980 \cdot c \cdot d \cdot B)$, where *c* is the protein concentration, B is the magnetic field (1 T), and *d* is the thickness of the sample (path length, 0.5 cm) [39,99,106–108]. The fluorescence emission spectra were recorded with a Jasco FP-6200 spectrofluorimeter with a quartz cuvette of 1 cm path length, using the following acquisition parameters: excitation wavelength 295 nm, bandwidth 5 nm, data pitch 1 nm, scan rate 250 nm/min. Following each CL addition, fluorescence spectra were recorded at 2 min time intervals, until two identical consecutive spectra were obtained.

2.4. Schemes of CL addition to ycc

For each protein, measurements were carried out in the presence of low (from 0.5 to 10) and high (from 5 to 60) CL/ycc molar ratios [39]. Spectra were recorded using CL/M80A ratios of: 0, 0.5, 1, 1.5, 2, 2.5, 3, 3.5, 4, 4.5, 5, 5.5, 6, 6.5, 7, 7.5, 8, 9, 10, and 0, 5, 10, 15, 20, 25, 30, 35, 40, 45, 50 and 60, respectively [39].

2.5. Dynamic light scattering measurements

Dynamic light scattering (DLS) measurements were performed with a Malvern Instruments Zetasizer Nano ZS. Data were collected using the SG and LA scheme in the presence of 5 μM M80A in 5 mM HEPES buffer at pH 7.0 [39]. The results are reported in terms of intensity distributions, where the area of the peak corresponding to each distribution is proportional to the intensity of scattered light. As previously reported

Table 1

Size of the liposomes observed in solution containing 5 μM ycc in 5 mM HEPES buffer at pH 7.0 in the presence of the same CL concentration used to study the CL-M80A interaction using low (0–10) CL/M80A molar ratios, obtained with small and gradual CL additions (SG scheme). The average liposome diameters and their relative contribution to the total liposomes population are extracted from the intensity distribution plots.

[CL]/ [ycc]	Average diameter species 1	Average diameter species 2	Average diameter species 3	Average diameter species 4	% species 1	% species 2	% species 3	% species 4
	(nm)	(nm)	(nm)	(nm)				
0	615			–	100			
1		47	205	–		14.1	85.9	–
2		68	164	5560		32.8	63.2	4
3		99	436	5210		52.3	44.7	3
4		119		5550		95.6		4.4
5		106		3560		97		3
6		92	487	3550		66.6	28	5.4
7		110		5550		95.7		4.3
8		76	449	4600		66.8	29	4.2
9		50	166	5300		52.7	46.2	1.1
10		104		4605		95.7		4.3

Table 2

Size of the liposomes observed in solution containing 5 μM ycc in 5 mM HEPES buffer at pH 7.0 in the presence of the same CL concentration used to study the CL-M80A interaction using low (0–60) CL/M80A molar ratios, obtained with small and gradual CL additions (LA scheme). The average liposome diameters and their relative contribution to the total liposomes population are extracted from the intensity distribution plots.

[CL]/ [ycc]	Average diameter species 1	Average diameter species 2	Average diameter species 3	Average diameter species 4	% species 1	% species 2	% species 3	% species 4
	(nm)	(nm)	(nm)	(nm)				
0	615				100			
5	597	54	–		17.6	82.4		
10	629	65	5193		87	9.3	3.7	
15	243	57	5450		21.3	77.2	1.5	
20	800	69	5280		19.3	78.1	2.6	
25		82	2000			74	26	
30		78	2100			84.8	15.2	
35		80	1796			78.3	21.7	
45		70	5390	367		72.7	4.1	23.2
55		108	4470	360		70		30

[39], in the absence of CL aggregates with diameters of 615 nm are observed (Tables 1 and 2).

It appears that both the SG and LA addition schemes result in solutions containing a mixture of two different liposome distributions (Table 1 and 2): one featuring an average diameter roughly lower than 200 nm and a second one with average diameter higher than 3000 nm, which is comparable to that of Giant Unilamellar Vesicles [109]. The latter liposomes have a higher contribution to the overall scattered light in the solutions obtained with the LA scheme, featuring high CL concentrations. However, it should be noted that the intensity of the scattered light is proportional to the sixth power of the liposome radius, resulting into an overestimation of the concentration of large liposomes (> 3000 nm). The aggregates with diameters of 600–800 nm observed for [CL]/[M80A] \leq 20 with the LA scheme (Table 2) most probably do not correspond to CL liposomes, since similar species are observed also in absence of CL.

3. Results

3.1. Absorption, MCD and CD spectra in the Soret region

The electronic absorption and MCD spectra of ferric M80A in the Soret region at pH 7 in the absence of CL (Figs. 1 and 2 and Table 1) match those reported previously [15,25,96,97,99,110]. The spectra indicate the presence of a prevailing 6-coordinate His/OH⁻ low spin (LS1) form [15,85,87,96,97,99,101,110,111], in equilibrium with a minor high-spin (HS1) form, revealed by the broad shoulder at 396 nm observed in the 2nd derivative absorption spectra (Figs. 1b and 2b and Table 1).

The CD signal associated to the Soret band has been widely used to probe for the structural changes in the heme environment [35,44,51,64,65,79,109,112], since a substantial part of the observed Cotton effect of the Soret band results from dipole-dipole coupling involving the $\pi \rightarrow \pi^*$ transitions of the heme and nearby protein chromophores as well as from non-planar deformations of the heme [44]. In particular, the negative component of the pronounced couplet typical of the native form of cytochromes *c* has been considered a probe of the environment on the Met80 side of the heme pocket and its decrease, or disappearance, has been associated with the formation of non-native protein conformers, involving the rupture of the Fe³⁺-Met80 axial bond [35,44,51,64,65,79,109,112]. The CD spectrum of M80A shows an intense peak at 403 nm (Figs. 1d and 2d), which is sensibly blue-shifted compared to the wt protein [35,51,64,65,79,109,112], and no trough, in agreement with the mutation-induced removal of the Fe³⁺-Met80 axial bond [110].

3.2. Near-UV CD spectra and fluorescence emission spectra

Both near-UV (250–330 nm) CD spectra and fluorescence emission spectra provide information on the protein environment surrounding Trp59, which is located in the heme crevice of folded cytochromes *c* [22,25,50,110]. Therefore, both techniques are extensively used to monitor the unfolding of cytochromes *c*, being particularly sensitive to changes in the overall folding [22,25,104,105,110,113–117].

The near-UV CD spectrum of wt ferric ycc contains a number of small positive bands between 250 and 265 nm, arising from tyrosine side chains [104] and porphyrin transitions [113], and two sharp negative bands at 282 and 289 nm, assigned to transitions involving the Trp59

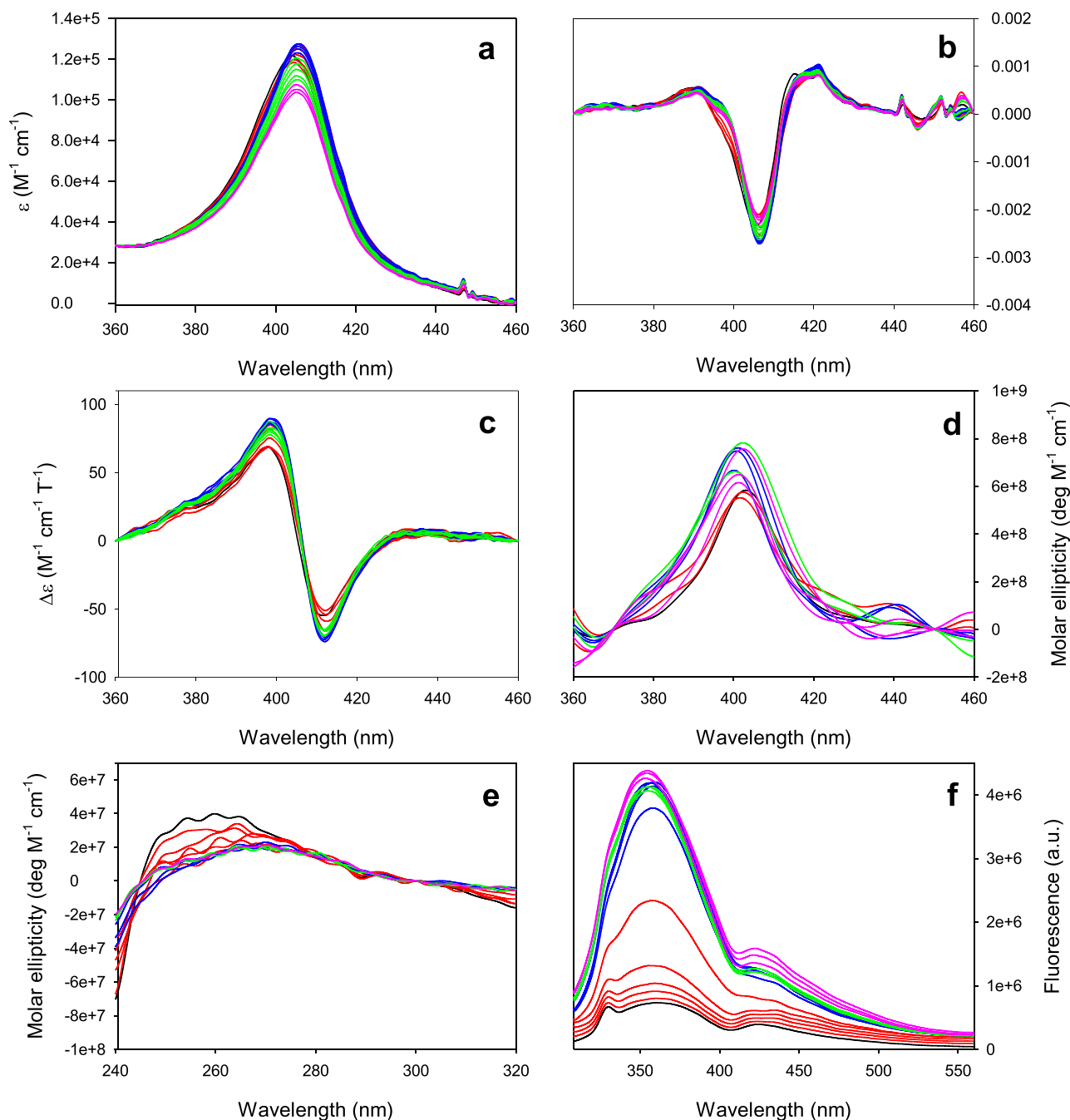


Fig. 1. (a) Electronic absorption spectra; (b) 2nd derivative electronic absorption spectra; (c) MCD spectra; (d) CD spectra in the Soret region; (e) near-UV CD spectra and (f) fluorescence emission spectra of the M80A mutant of *S. cerevisiae* iso-1 ferricytochrome c in 5 mM Hepes buffer at pH 7 for [CL]/[M80A] 0–10.0. Initial protein concentration was 5 μ M. [CL]/[M80A] = 0.0, black; [CL]/[M80A] = 0.5, 1.0, 1.5, 2.0, 2.5, red; [CL]/[M80A] = 3.0, 3.5, 4.0, 4.5, 5.0, blue; [CL]/[M80A] = 5.5, 6.0, 6.5, 7.0, 7.5, green; [CL]/[M80A] = 8.0, 9.0, 10.0, pink. (For interpretation of the references to colour in this figure legend, the reader is referred to the web version of this article.)

side chain (Figs. 1e and 2e) [22,104,113]. The fluorescence emission spectrum of mitochondrial cytochromes c shows high-intensity and low-intensity bands, identified as F and P bands, respectively [79,118]. The former is due to the fluorescence emission of Trp59, whereas the origin of the phosphorescence-like P-band has not yet been identified [79,118]. In folded cytochrome c, Trp59 fluorescence emission is quenched by heme, but sharply increases when the residue moves away from the metal center, due to protein unfolding [22,50,51,65]. Moreover, the location of fluorescence peak is sensitive to the polarity of the environment surrounding Trp59 [22,50,51,65,79,118].

The quenching of the Trp59 fluorescence emission observed for the M80A variant (Figs. 1f and 2f) and the similarity of its near-UV CD spectrum to that of wt ycc indicates that deletion of axial Met80 ligand does not sensibly modify protein folding [22,104,105,110]. On the other hand, the significant red shift (~ 30 nm) of the fluorescence emission maximum compared to wt suggests an enhanced polarity of the Trp59 environment in the mutant, likely as the result of an increased solvent accessibility following removal the axial Met80 [22,51,65,79,110,118].

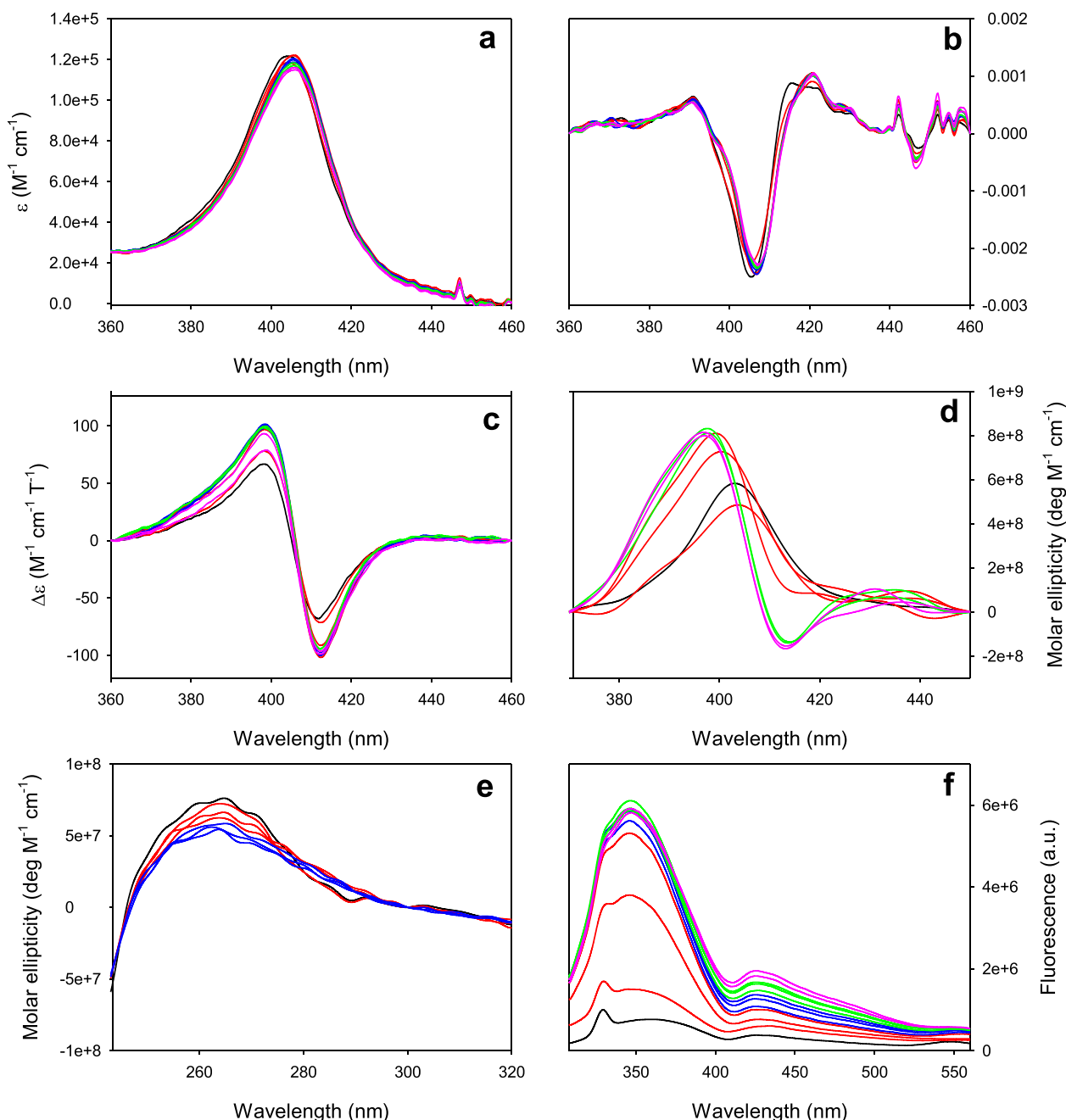


Fig. 2. (a) Electronic absorption spectra; (b) 2nd derivative electronic absorption spectra; (c) MCD spectra; (d) CD spectra in the Soret region; (e) near-UV CD spectra and (f) fluorescence emission spectra of the M80A mutant of *S. cerevisiae* iso-1 ferricytochrome *c* in 5 mM Hepes buffer at pH 7 for [CL]/[M80A] 60.0. Initial protein concentration was 5 μ M. [CL]/[M80A] = 0.0, black; [CL]/[M80A] = 5.0, 10.0, 15.0, red; [CL]/[M80A] = 20.0, 25.0, 30.0, blue; [CL]/[M80A] = 35.0, 40.0, 45.0, green; [CL]/[M80A] = 50.0, 60.0, pink. (For interpretation of the references to colour in this figure legend, the reader is referred to the web version of this article.)

3.3. Effects of CL addition on the absorption, MCD, CD and fluorescence emission spectra of M80A

3.3.1. Low CL/M80A molar ratios (from 0.5 to 10) obtained with small and gradual CL additions (“SG scheme”)

3.3.1.1. Absorption, MCD and CD spectra in the Soret zone. Upon addition of small increasing concentrations of CL, the Soret band in the absorption spectra and the single trough in the corresponding 2nd derivative spectra redshift by 1–2 nm (Fig. 1a,b and Table 3), whereas the broad shoulder observed in the 2nd derivative spectra around 397 nm disappears for a [CL]/[M80A] ratio of 4.0 and is replaced by new shoulder at 395 nm at higher [CL]/[M80A] ratios (Fig. 1b and Table 3).

An isosbestic point is observed at 401 nm for [CL]/[M80A] ratios between 1 and 4 (Fig. 1a). The S-shaped MCD signal associated with the Soret band slightly redshift (Fig. 1c and Table 3), retaining its symmetrical shape. An isodichroic point at 407 nm is observed for [CL]/[M80A] ratios between 1 and 3.5 and above 4.5, respectively.

Both the Soret band intensity and the peak-to-trough distance of the corresponding MCD signal increase up to a [CL]/[M80A] ratio of 3.5 and decreases upon further CL addition (Fig. 3a,b). These spectral changes indicate that the major low-spin His/OH⁻-ligated form (LS1_{M80A}) and the minor high-spin form (HS1_{M80A}) observed in the absence of CL both transform into a second LS conformer (LS2_{M80A}) for [CL]/[M80A] ratios up to about 3.5–4.0 (Table 4). The spectroscopic features of LS2_{M80A} are closely similar to those of the His/His axially coordinated conformer of

Table 3

Wavelengths of the relevant spectral features of the UV-Vis, MCD, CD and fluorescence emission spectra for the M80A mutant of *Saccharomyces cerevisiae* iso-1 cytochrome *c* in the presence of low and high CL/M80A molar ratios.

Low CL/M80A molar ratios									
[CL]/[M80A]	Absorption		MCD			CD		Fluorescence emission	
	Soret	2nd derivative	peak	trough	zerocross	peak	trough		
0	404	406, 397 (sh)	397	412	405	403	–		360
3.5	406	407	398	413	406	399	–		358
5.5	406	407, 395 (sh)	398	413	406	402	–		355
10	405	407, 395 (sh)	398	413	406	401	–		354
High CL/M80A molar ratios									
[CL]/[M80A]	Absorption		MCD			CD		Fluorescence emission	
	Soret	2nd derivative	peak	trough	zerocross	peak	trough		
0	404	406, 397 (sh)	397	412	405	403	–		360
5.0	404	406, 397 (sh)	398	413	406	404	–		346
10.0	405	406, 397 (sh)	398	413	406	401	–		346
15.0	406	407	398	413	406	399	–		346
20.0	406	407	398	413	406	399	414		346
60.0	406	407, 397 (sh)	398	413	406	398	413		347

the M80A mutant observed in the presence of high urea concentrations [25]. This suggests that upon interaction with CL the M80A variant undergoes the same axial ligand swapping to a His/His axially ligated form, observed for wt ycc and its KtoA mutants in the presence of similar [CL]/[M80A] ratios (Table 4) [39]. The monophasic increase in the Soret band intensity and in the peak-to-trough distance of the corresponding MCD signal observed for [CL]/[M80A] ratios up to 3.5 (Fig. 3a,b) suggests that formation of $LS2_{M80A}$ occurs in a single step, in contrast to the two-step process observed for wt cytc [39]. In the presence of [CL]/[M80A] ratios above 5.5, the $LS2_{M80A}$ species transforms into a new high-spin form ($HS2_{M80A}$), whose spectroscopic properties apparently differ from those of the $HS1_{M80A}$ conformer (Table 4). Unfortunately, the low protein concentration (5 μ M) required to achieve high CL/cytochrome *c* molar ratios prevented an analysis of the charge transfer bands typical of HS ferric hemes, observed in the 600–650 nm region [119–121].

Increasing concentrations of CL sensibly alter both the position and intensity of the CD signal associated to the Soret band, without significantly modifying its shape (Fig. 1d). Initially, the single peak blue-shifts to 400 nm (up to a [CL]/[M80A] ratio of 3.5), but then moves back to 401 nm at [CL]/[M80A] = 10.0, whereas its intensity sensibly increases up to a molar ratio of 4.5 and decreases at ratios higher than 6.0 (Fig. 1d). This behavior parallels that of the corresponding UV-vis and MCD spectra.

3.3.1.2. Near-UV CD spectra and fluorescence emission spectra. Addition of small increasing concentrations of CL simplifies the near-UV CD spectrum of the M80A variant (Fig. 1e), as the two sharp negative bands at 282 and 289 nm and the three maxima at 255, 260 and 265 nm progressively decrease in intensity and disappear at [CL]/[M80A] ratios above 3.0. These changes suggest that disruption of the tight packing of core residues occurs in the mutant upon increasing [CL]/[M80A] ratios up to 3.0. No significant changes are observed at higher ratios.

The Trp59 fluorescence emission of M80A significantly increases up to [CL]/[M80A] ratio of 4.0 (Figs. 1e and 3c), indicating that upon CL binding the residue moves away from the heme [50,51,65] due to the progressive loss of the protein tertiary structure. The observed increase of the Trp59 fluorescence emission show the same monophasic behavior observed for the Soret band and the corresponding MCD signal (Fig. 3c). No significant changes are observed upon further CL addition. Interestingly, upon increasing [CL]/[M80A] ratios the peak emission slightly blueshifts, from 360 nm ([CL]/[M80A] = 0) to 355 nm ([CL]/[M80A] \geq 6) (Fig. 1f and Table 1), consistent with Trp59 experiencing a slightly less polar environment.

3.3.2. High CL/M80A molar ratios (from 5 to 60) obtained with large CL additions (LA scheme)

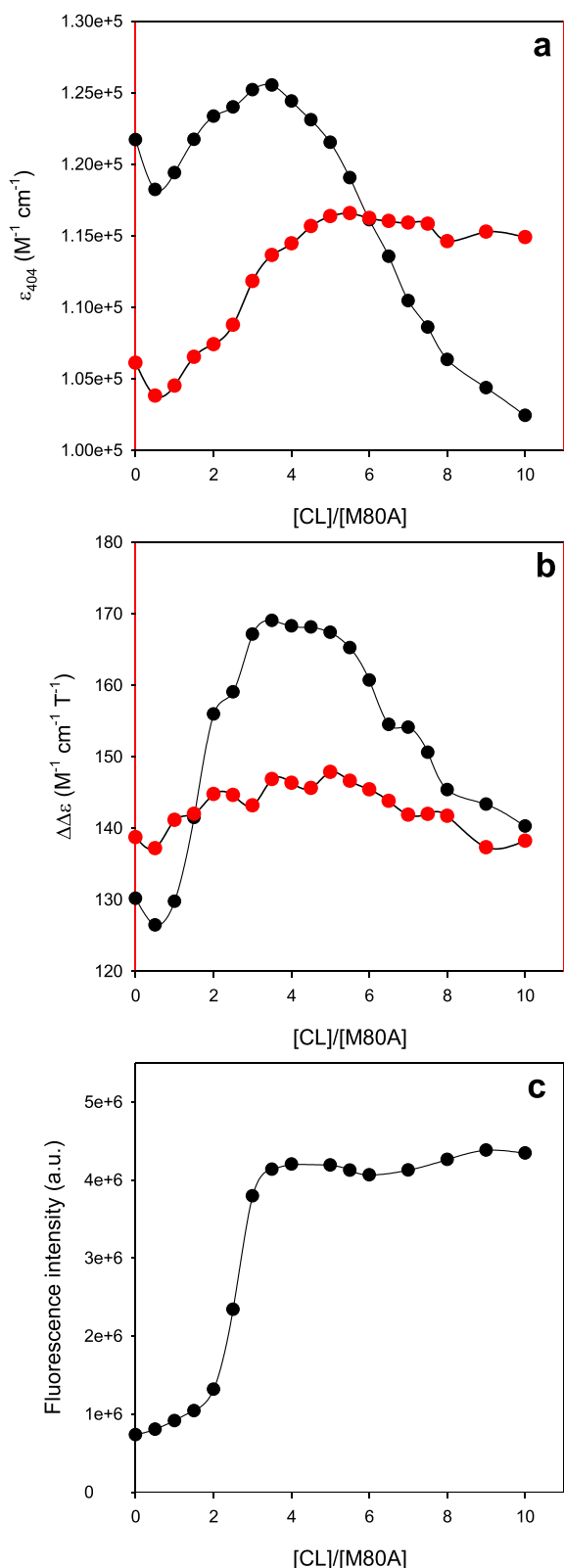
3.3.2.1. Absorption, MCD and CD spectra in the Soret zone. Upon increasing the [CL]/[M80A] ratio by 5 or 10 unit steps, from an initial value of 5 to a final value of 60, the Soret band and the single trough observed in 2nd derivative UV-Vis spectra red shifts by 1–2 nm (Fig. 2a, b and Table 3). The broad shoulder observed in the 2nd derivative spectra around 397 nm disappears for [CL]/[M80A] of 10.0 and a new shoulder appears at higher ratios (Fig. 2a,b and Table 3). The S-shaped MCD signal associated with the Soret band slightly redshifts (Fig. 2c and Table 3), retaining its symmetrical shape. An isodichroic point at 404 nm is observed for [CL]/[M80A] \geq 10.0 (Fig. 2c).

The Soret band intensity and the peak-to-trough distance of the corresponding MCD signal increase up to [CL]/[M80A] ratios of 15.0 and decrease at higher ratios (Fig. 4a,b). These spectral changes indicate that the native LS His/OH[−] ligated form ($LS1_{M80A}$) and the minor high-spin form ($HS1_{M80A}$) transform into a second LS conformer ($LS2_{M80A-hr}$, where *hr* stands for [CL]/[M80A] high ratios), which is completely formed at a molar ratio of 15 (Table 4), whose spectroscopic electronic and MCD spectra in the Soret region are closely similar to those of $LS2_{M80A}$, indicating the same bis-His axial heme coordination. The appearance of shoulder at 397 nm in the 2nd derivative spectra (Fig. 2b) and the concomitant decrease of the intensity of the Soret band and of the corresponding MCD signal (Figs. 2a,c and Figs. 4a,b) indicates that a limited amount of a high-spin species ($HS2_{M80A-hr}$) is formed for molar ratios above 15 (Table 2) [35,49,53,69,81,122].

CL addition strongly affects both the shape and the intensity of the CD signal associated to the Soret band (Figs. 2d and Table 3). The peak becomes more intense and blue-shifts from 403 to 397 nm up to a [CL]/[M80A] ratio of 25.0, while a deep trough at 414 nm appears at a molar ratio of 20.0 (Figs. 2d and Table 3), as previously reported for wt ycc and some of its KtoA variants [51]. No significant changes occur upon further CL addition.

3.3.2.2. Near-UV CD spectra and fluorescence emission spectra. The two sharp negative bands at 282 and 289 nm disappear at [CL]/[M80A] ratios above 5.0 and the three maxima between 255 and 265 nm progressively decrease in intensity (Figs. 2c). These spectral features suggest that the tight packing of core residues of M80A is disrupted at [CL]/[M80A] ratios above 10.0.

The emission fluorescence spectra of M80A show a relevant increase of the Trp59 fluorescence coupled to a significant blue shift of the peak emission (from 360 to 346 nm) up to a [CL]/[M80A] ratio of 10.0. As limited changes are observed at higher CL concentration (Figs. 2f and Table 3), the loss of M80A tertiary structure is almost complete at [CL]/



(caption on next column)

Fig. 3. Changes in a) the extinction coefficient of the maximum of the Soret band, b) the peak-to-trough difference in the MCD signal associated with the Soret band and c) the intensity of the fluorescence emission observed for [CL]/[M80A] from 0 to 10.0 for the M80A mutant of *S. cerevisiae* iso-1 ferricytochrome *c*. Protein dilution after each CL addition was considered when calculating the ϵ_{404} and $\Delta\Delta\epsilon$ values as well as the changes in fluorescence emission. Solid lines are simply drawn through the data point to clarify the CL-induced changes and do not correspond to least squares fits. The red plots reported in a) and b) describe the changes in the extinction coefficient of the maximum of the Soret band at 407 nm and the peak-to-trough difference in the MCD signal associated with the Soret band observed for wild type *S. cerevisiae* iso-1 ferricytochrome *c*, respectively (from ref. [39]). (For interpretation of the references to colour in this figure legend, the reader is referred to the web version of this article.)

[M80A] = 10.0. Moreover, the greater blueshift of the peak emission (15 nm) compared to that observed with the SG addition scheme (5 nm) indicates that, upon increasing the CL/M80A molar ratio by 5 or 10 unit steps, Trp59 moves to a much less polar environment.

4. Discussion

The Met80 belongs to the least stable portion of cytc, usually indicated as *red foldon* [18,123–126]. Although the Fe – S(Met80) bond forms in the last phases of protein folding and dissociates during the early steps of unfolding [18,123–126], it significantly contributes to the overall stability of the 3D structure of wt cytc. Indeed, its deletion severely reduces the resistance of M80A to urea-induced unfolding compared to the wt protein, lowering the $\Delta G_u^{H_2O}$ for the protein both in solution and immobilized on negatively charged SAMs that mimic the IMM [24,25]. Since the axial coordination of the heme iron heavily influences the reactivity of cytc [1–3,5–8,29,30,37,44], the Met80-Fe bond is the molecular trigger controlling the role of mitochondrial cytochrome *c* *in vivo*. Indeed, its involvement in the mitochondrial ET chain is strictly related to the presence of the Fe – S(Met80) bond, since the positive reduction potential of the Fe(III/II) couple in native cytc mainly depends on the selective stabilization of the ferrous form by the soft sulfur donor of Met80 [16,90,127]. On the other hand, cleavage of the Fe – S(Met80) bond, due to protein unfolding or Met80 deletion, transforms cytc into an effective oxidoreductase possessing significant pseudo-peroxidase and pseudo-nitrite reductase activities, essential to its pro-apoptotic and detoxifying roles [1,2,4,5,8,29,30,37]. It is therefore important to single out the influence of the Fe – M80 bond on the cytc-CL interaction, since its cleavage is invariably observed upon cytc binding to CL-containing membranes.


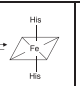
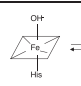
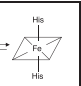
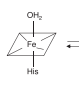
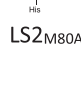
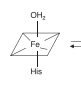
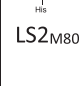


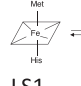
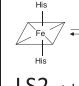
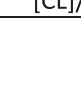
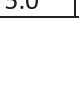
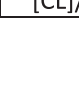
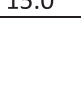
The significant spectral changes induced by increasing CL concentrations demonstrate that cardiolipin specifically interacts with M80A, remarkably affecting both its overall conformation and the electronic properties of the heme, as previously observed for wt ycc and some KtoA variants [39]. Hence, deletion of the Fe – M80 bond does not prevent cytc binding to CL-containing membranes.

4.1.1. Low CL/M80A molar ratios (from 0.5 to 10) obtained with small and gradual CL additions (“SG scheme”)

Upon small and gradual CL additions, wt cytc undergoes an axial ligand swapping for [CL]/[cytc] ratios up to 5.0, resulting in a low-spin His/His axially coordinated conformer ($LS2_{wt}$) [39]. Formation of $LS2_{wt}$ is a two-step process, as expected according to the “extended lipid anchorage” model, which assumes that after electrostatic interaction with surface lysines, one or two CL acyl chain insert into hydrophobic channels of cytc connecting the protein surface to the heme cavity [8,30,34,70,72–74]. This event forces cytc into a more open conformation by disrupting the hydrogen bond connecting His26 and Glu44

Table 4

CL/M80A molar ratios at which changes in the axial ligation and spin state of the ferric heme center occur for the M80A mutant and the wt form of *Saccharomyces cerevisiae* iso-1 cytochrome *c*.

	Low [CL]/[cytc] ratios (SG Scheme)		High [CL]/[cytc] ratios (LA Scheme)	
M80A				
	LS1 _{M80A}	LS2 _{M80A}	LS1 _{M80A}	LS2 _{M80A-hr}
				
	HS1 _{M80A}	HS2 _{M80A}	HS1 _{M80A}	HS2 _{M80A-hr}
	[CL]/[M80A] ≤ 3.5	[CL]/[M80A] ≥ 5.5	[CL]/[M80A] ≤ 15.0	[CL]/[M80A] ≥ 15.0
wt ^a				
	LS1 _{wt}	LS2 _{wt}	LS1 _{wt}	LS2 _{wt-hr}
				
	LS2 _{wt}	HS1 _{wt}	LS2 _{wt-hr}	HS1 _{wt-hr}
	[CL]/[ycc] ≤ 5.0	[CL]/[ycc] ≥ 5.0	[CL]/[ycc] ≤ 15.0	[CL]/[ycc] ≥ 15.0

^a From ref. [39].

(ycc) or Pro44 (horse and human cytc) as well as the Fe – S(Met80) bond [1,29,37,39,43,64,128,129]. Moreover, a small amount of a high spin form (HS1_{wt}) is observed in the presence of [CL]/[cytc] ratios ≥ 5.0 [39].

The overall behavior of M80A in the same experimental conditions is reminiscent of that of wt ycc (Table 4), since the observed spectral changes indicate that formation of a His/His axially coordinated LS2_{M80A} form similar to LS2_{wt} occurs for [CL]/[M80A] ≤ 3.5 together with disruption of the tight packing of the core residues and a reorganization of the heme crevice. However, formation of the LS2_{M80A} species occurs at lower [CL]/[M80A] ratios compared to LS2_{wt} and is accomplished in a single step (Fig. 3 and Table 4). Hence, deletion of the Fe – M80 bond increases the affinity of M80A for CL and alters its binding mechanism compared to the wt protein. Interestingly, a similar effect was observed for the K73A/K79A, K72A/K79A and K72A/K73A/K79A variants and was attributed to an easier conversion into a more open conformation, due to the mutation-induced cleavage of the H-bond between the N_ε of His26 and the backbone oxygen of Glu44 [39,128,129].

Both the increased affinity for CL and the altered binding mechanism of M80A fit with its lower $\Delta G^{\circ-H_2O}$ compared to wt ycc, since an easier protein unfolding would facilitate heme axial ligand swapping upon CL binding as well as the transition to a more open conformation as a consequence of insertion of CL acyl chains into the protein hydrophobic core, as predicted by the “extended lipid anchorage” model. The structural effects of the M80A mutation [111] should not significantly affect the electrostatic interaction between the negatively charged groups of CL and the surface lysines, as the overall fold of M80A is superimposable to that of the wt protein (Fig. 5), whereas insertion of CL acyl chains into the protein hydrophobic core should be facilitated, compared to the wt protein. Indeed, the replacement of the axial Met80 with an alanine produces a wide cavity on the distal side of the heme [111], which greatly increases its accessibility compared to the wt protein and therefore can easily accommodate one of the CL acyl chains (Fig. 5). Insertion of the CL acyl chain into the M80A core would reduce the polarity of the heme crevice, resulting in the 5-nm red shift (from 360 to 355 nm) of the Trp59 fluorescence emission observed upon CL binding (Fig. 1f and Table 1). Moreover, inspection of the 3D structure of M80A reveals that the H-bond between the N_ε of His26 and the backbone oxygen of Glu44 is cleaved, as in the above mentioned KtoA variants [111]. These mutation-induced structural effects should result in an easier insertion of the CL acyl chains into the protein hydrophobic core

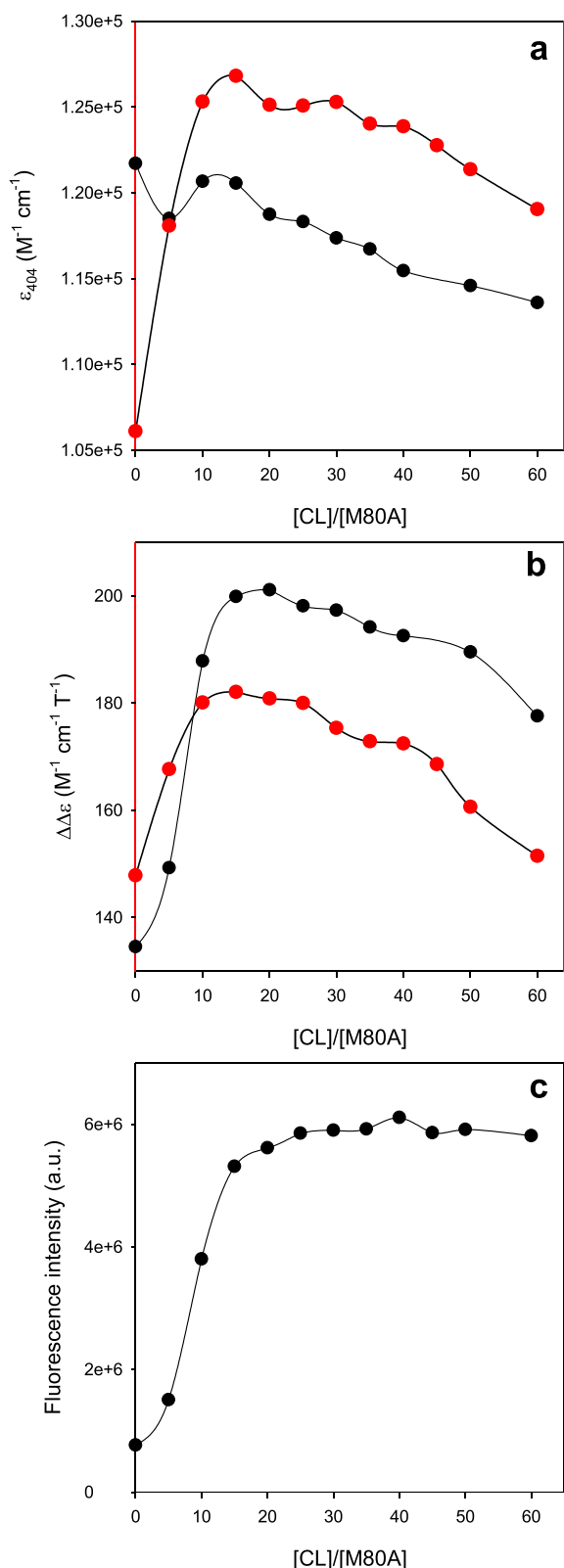
compared to wt ycc, enhancing the affinity of M80A for CL to such an extent that the preliminary electrostatic step and CL insertion to form LS2_{M80A} would coalesce into a single-step process.

4.1.2. High CL/M80A molar ratios (from 5 to 60) obtained with large and abrupt CL additions (“LA scheme”)

The spectral changes observed for M80A upon large additions of CL indicate that for [CL]/[M80A] lower than 15, the native LS His/OH⁻ ligated form (LS1_{M80A}) and the minor high-spin form (HS1_{M80A}) transform into a new LS form (LS2_{M80A-hr}), featuring the same bis-His axial coordination for the heme group as LS2_{M80A} (Table 4). Axial ligand swapping is accompanied by disruption of the tight packing of the core residues and the loss of the protein tertiary structure. Hence, formation of LS2_{M80A-hr} conformer occurs at larger CL/M80A molar ratios compared to the LS2_{M80A} obtained with the SG scheme (Table 4), which is completely formed for [CL]/[M80A] = 3.5. Indeed, the electronic, MCD, near-UV CD and fluorescence emission spectra recorded at [CL]/[M80A] = 5 upon a single and large CL addition are very similar to that of the native LS1_{M80A} His/OH⁻ ligated conformer (Table 3), indicating that limited axial ligand swapping and disruption of the protein fold occur, compared to those observed when the same CL/cytc molar ratio is obtained more gradually and with smaller CL additions. Hence, it turns out that the LA addition scheme affects the structure of the M80A mutant less efficiently than the SG addition scheme, as previously observed for wt ycc and some KtoA mutants [39].

Comparison of the Trp59 fluorescence emission spectra in the presence of [CL]/[M80A] ratios of 5 and 10 (Figs. 1f and 2f) reveals that the LA addition scheme induces a much greater blue shift (from 360 to 346 nm) of the emission peak compared to the SG addition scheme (from 360 to 355 nm) (Figs. 1f and 2f and Table 1), indicating that in the former case Trp59 moves to a much less polar environment. Therefore, it appears that, although LS2_{M80A-hr} and LS2_{M80A} share the same bis-His heme axial coordination, the CL-bound M80A mutant adopts different conformations depending on the CL addition scheme, indicating that the effect of CL binding on the overall structure of ycc is affected not only by the CL/cytc ratio, but also by the way in which such ratio is obtained.

The available data indicate that both wt and M80A, under the LA scheme, interact with CL mainly through electrostatic interaction followed by anchoring through the peripheral binding model [41,45,46,62,65,67,76,77], which implies a progressive shift from the C to the E form as cytc crowding on the membrane surface decreases



(caption on next column)

Fig. 4. Changes in a) the extinction coefficient of the maximum of the Soret band, b) the peak-to-trough difference in the MCD signal associated with the Soret band and c) the intensity of the fluorescence emission observed for [CL]/[M80A] from 0 to 60.0 for the M80A mutant of *S. cerevisiae* iso-1 ferricytochrome *c*. Protein dilution after each CL addition was considered when calculating the ϵ_{404} and $\Delta\Delta\epsilon$ values as well as the changes in fluorescence emission. Solid lines are simply drawn through the data point to clarify the CL-induced changes and do not correspond to least squares fits. The red plots reported in a) and b) describe the changes in the extinction coefficient of the maximum of the Soret band at 407 nm and the peak-to-trough difference in the MCD signal associated with the Soret band observed for wild type *S. cerevisiae* iso-1 ferricytochrome *c*, respectively (from ref. [39]). (For interpretation of the references to colour in this figure legend, the reader is referred to the web version of this article.)

[45,51,65,78,79]. Indeed, high CL concentrations in lipid layers and large available membrane surface areas induces massive cytc unfolding [5,28,39,51,65,79,109]. This is supported by the dynamic light scattering data, which show that under the LA scheme, a significant amount of CL liposomes comparable to Giant Unilamellar Vesicles are detected in the presence of high CL concentration (Table 4). As previously noted [39], the observed behavior is consistent with the two consecutive intramolecular structural rearrangements occurring upon binding of ycc on the surface of 100% CL liposomes at slightly alkaline pH values, which involve a small heme-centered structural rearrangement followed by partial protein unfolding at higher CL/cytc ratios [50,51,65]. In principle, the two consecutive intramolecular structural rearrangements could correspond to the transition to the $LS2_{M80A-hr}$ and the conversion of $LS2_{M80A-hr}$ to $HS2_{M80A-hr}$, respectively.

The higher efficiency of the SG addition scheme in inducing axial ligand swapping and disruption of the protein fold is not consistent with the peripheral binding model, since the higher surface crowding expected in the presence of small [CL]/[M80A] should result in limited structural perturbations of M80A [5,51,65,79]. Therefore, it appears that under the SG scheme a different M80A-CL binding mechanism is operative, possibly the extended lipid anchorage model [29,35,39,49,73,75].

Indeed, the structural transformation occurring to CL-containing large unilamellar vesicles at increasing cytc/lipid ratio are indicative of a multi-phase process, involving the interaction of the protein with the lipid polar heads, its lipid anchorage on the membrane surface and an order/disorder transition of the CL acyl chains [57].

The close similarity between the wavelength of the Trp59 emission peak obtained for M80A with the LA CL addition scheme and those reported for *wt* and mutated ycc bound to CL-containing vesicles [50,51,65] indicates that their heme environments feature similar polarities, which are intermediate between the highly polar environment of the folded M80A and the largely hydrophobic environment of the folded *wt* protein. Therefore, it appears that upon binding to large CL vesicles, *wt* ycc and M80A adopt similar conformations. This hypothesis is further confirmed by the appearance of the deep trough at 414 nm in the Soret CD spectra for [CL]/[M80A] \geq 20.0 (Fig. 2d and Table 3), which matches the behavior reported for *wt* ycc and some of its KtoA mutants in similar conditions [51]. Since the Soret CD spectrum of cytochrome *c* is heavily influenced by the internal electric field of the protein and by associated vibronic perturbations [5,44,130,131], the above-mentioned similarities strongly suggest that M80A and *wt* ycc feature similar heme environments in the presence of high CL to protein ratios. Since the CD couplet results from the splitting of the excited B-state [5,44,130,131], its presence indicates a rather asymmetric heme environment in both cases [51].

5. Conclusions

This study sought to expand our understanding of the complex interplay of molecular factors controlling the interaction between cytc

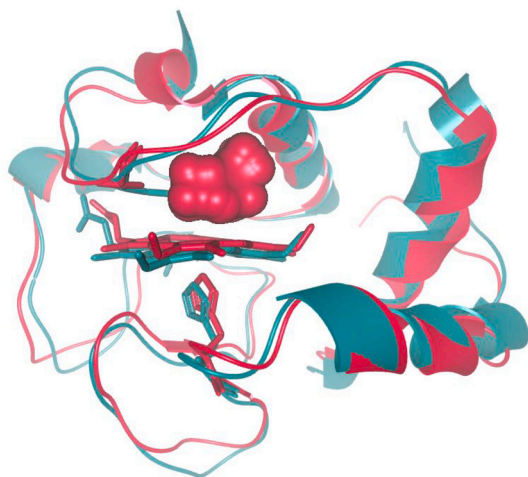


Fig. 5. 3D structures of M80A mutant (PDB 1FHB, red) and wt *S. cerevisiae* iso-1 cytochrome *c* (PDB 1YCC, green). The heme group, His18 and Ala80 in the M80A mutant are represented as red sticks, while the heme group, His18 and Met80 in the wt protein are represented as green sticks. The distal cavity resulting from the M80A mutation is reported in red. (For interpretation of the references to colour in this figure legend, the reader is referred to the web version of this article.)

and CL, by focusing on the role of the Fe – M80 axial bond. The comprehensive spectroscopic evidence presented demonstrates that M80A specifically binds to CL-containing membranes. Most importantly, the higher heme accessibility and lower structural stability of the mutant do not result in a significant alteration of the observed protein unfolding and heme ligation pattern compared to the wt protein in the same experimental conditions, thereby indicating that the Fe – M80 axial bond exerts a limited influence on the cytc-CL interaction mechanism, which in turn is heavily dependent on the way CL and cytc are mixed. Hence, the molecular determinants of the cytc-CL interactions in the *in vitro* conditions employed are located outside the heme environment. Apparently the most notable effect of the M80A mutation is an easier insertion of the CL acyl chains into the protein hydrophobic core at low CL/cytc compared to wt ycc, resulting in an enhanced affinity of the mutant for CL.

Author statement

Data will be made available on request.

CRedit authorship contribution statement

Alessandro Paradisi: Investigation, Data curation. **Marzia Bellei:** Investigation, Data curation. **Carlo Augusto Bortolotti:** Writing – review & editing, Formal analysis. **Giulia Di Rocco:** Writing – review & editing, Formal analysis. **Antonio Ranieri:** Writing – review & editing, Investigation. **Marco Borsari:** Writing – review & editing, Writing – original draft, Methodology, Conceptualization. **Marco Sola:** Writing – review & editing, Methodology, Conceptualization. **Gianantonio Battistuzzi:** Writing – review & editing, Writing – original draft, Methodology, Funding acquisition, Conceptualization.

Declaration of Competing Interest

The authors declare that they have no known competing financial interests or personal relationships that could have appeared to influence the work reported in this paper.

Data availability

Data will be made available on request.

Acknowledgements

This work was supported by the University of Modena and Reggio Emilia FAR 2021–DSCG funding program.

References

- [1] D. Alvarez-Paggi, L. Hannibal, M.A. Castro, S. Oviedo-Rouco, V. Demicheli, V. Tórtora, F. Tomasina, R. Radi, D.H. Murgida, Multifunctional cytochrome *c*: learning new tricks from an old dog, *Chem. Rev.* 117 (2017) 13382–13460, <https://doi.org/10.1021/acs.chemrev.7b00257>.
- [2] S. Zaidi, M.I. Hassan, A. Islam, F. Ahmad, The role of key residues in structure, function, and stability of cytochrome-*c*, *Cell. Mol. Life Sci.* 71 (2014) 229–255, <https://doi.org/10.1007/s00018-013-1341-1>.
- [3] I. Bertini, G. Cavallaro, A. Rosato, Cytochrome *c*: occurrence and functions, *Chem. Rev.* 106 (2006) 90–115, <https://doi.org/10.1021/cr050241v>.
- [4] M. Hüttemann, P. Pecina, M. Rainbolt, T.H. Sanderson, V.E. Kagan, L. Samavati, J.W. Doan, I. Lee, The multiple functions of cytochrome *c* and their regulation in life and death decisions of the mammalian cell: from respiration to apoptosis, *Mitochondrion*. 11 (2011) 369–381, <https://doi.org/10.1016/j.mito.2011.01.010>.
- [5] R. Schweitzer-Stenner, Relating the multi-functionality of cytochrome *c* to membrane binding and structural conversion, *Biophys. Rev.* 10 (2018) 1151–1185, <https://doi.org/10.1007/s12551-018-0409-4>.
- [6] G.W. Moore, G. Rk, Pettigrew, *Cytochromes c. Evolutionary, Structural, and Physicochemical Aspects*, Springer-Verlag, Berlin, Germany, 1990.
- [7] R. A. Mauk, in: A.G. Scott (Ed.), *Cytochrome c - A Multidisciplinary Approach*, University Science Books, Sausalito, CA, 1996.
- [8] R. Santucci, F. Sinibaldi, P. Cozza, F. Polticelli, L. Fiorucci, Cytochrome *c*: an extreme multifunctional protein with a key role in cell fate, *Int. J. Biol. Macromol.* 136 (2019) 1237–1246, <https://doi.org/10.1016/j.ijbiomac.2019.06.180>.
- [9] S. Hirota, S. Nagao, New aspects of cytochrome *c*: 3D domain swapping, membrane interaction, peroxidase activity, and Met80 sulfoxide modification, *Bull. Chem. Soc. Jpn.* 94 (2021) 170–182, <https://doi.org/10.1246/BCSJ.20200272>.
- [10] S. Neya, M. Suzuki, T. Hoshino, H. Ode, K. Imai, T. Komatsu, A. Ikezaki, M. Nakamura, Y. Furutani, H. Kandorib, Molecular insight into intrinsic heme distortion in ligand binding in hemoprotein, *Biochemistry*. 49 (2010) 5642–5650, <https://doi.org/10.1021/bi1003553>.
- [11] J. Liu, S. Chakraborty, P. Hosseinzadeh, Y. Yu, S. Tian, I. Petrik, A. Bhagi, Y. Lu, Metalloproteins containing cytochrome, iron-sulfur, or copper redox centers, *Chem. Rev.* 114 (2014) 4366–4469, <https://doi.org/10.1021/cr400479b>.
- [12] G. Battistuzzi, M. Borsari, M. Sola, F. Francia, Redox thermodynamics of the native and alkaline forms of eukaryotic and bacterial class I cytochromes *c*, *Biochemistry*. 36 (1997) 16247–16258, <https://doi.org/10.1021/bi971535g>.
- [13] G. Battistuzzi, M. Borsari, M. Sola, Medium and temperature effects on the redox chemistry of Cytochromec, *Eur. J. Inorg. Chem.* 2001 (2001) 2989–3004, [https://doi.org/10.1002/1099-0682\(200112\)2001:12<2989::AID-EJIC2989>3.0.CO;2-E](https://doi.org/10.1002/1099-0682(200112)2001:12<2989::AID-EJIC2989>3.0.CO;2-E).
- [14] G. Battistuzzi, M. Borsari, M. Sola, Redox properties of cytochrome *c*, antioxidants redox, *Signal.* 3 (2001) 279–291, <https://doi.org/10.1089/152308601300185232>.
- [15] L. Lancellotti, M. Borsari, A. Bonifacio, C.A. Bortolotti, G. Di Rocco, S. Casalini, A. Ranieri, G. Battistuzzi, M. Sola, Adsorbing surface strongly influences the pseudoperoxidase and nitrite reductase activity of electrode-bound yeast cytochrome *c*. The effect of hydrophobic immobilization, *Bioelectrochemistry*. 136 (2020), 107628, <https://doi.org/10.1016/j.bioelechem.2020.107628>.
- [16] G. Di Rocco, G. Battistuzzi, M. Borsari, C.A. Bortolotti, A. Ranieri, M. Sola, The enthalpic and entropic terms of the reduction potential of metalloproteins: determinants and interplay, *Coord. Chem. Rev.* 445 (2021), 214071, <https://doi.org/10.1016/j.ccr.2021.214071>.
- [17] S.W. Englander, T.R. Sosnick, L.C. Mayne, M. Shtilerman, P.X. Qi, Y. Bai, Fast and slow folding in cytochrome *c*, *Acc. Chem. Res.* 31 (1998) 737–744, <https://doi.org/10.1021/ar970085h>.
- [18] M.M.G. Krishna, Y. Lin, J.N. Rumbley, S.W. Englander, Cooperative omega loops in cytochrome *c*: role in folding and function, *J. Mol. Biol.* 331 (2003) 29–36, [https://doi.org/10.1016/S0022-2836\(03\)00697-1](https://doi.org/10.1016/S0022-2836(03)00697-1).
- [19] M.G. Duncan, M.D. Williams, B.E. Bowler, Compressing the free energy range of substrate stabilities in iso-1-cytochrome *c*, *Protein Sci.* 18 (2009) 1155–1164, <https://doi.org/10.1002/pro.120>.
- [20] M.M. Cherney, B.E. Bowler, Protein dynamics and function: making new strides with an old warhorse, the alkaline conformational transition of cytochrome *c*, *Coord. Chem. Rev.* 255 (2011) 664–677, <https://doi.org/10.1016/j.ccr.2010.09.014>.
- [21] S. Baddam, B.E. Bowler, Thermodynamics and kinetics of formation of the alkaline state of a Lys 79→ala/Lys 73→his variant of iso-1-cytochrome *c*, *Biochemistry*. 44 (2005) 14956–14968, <https://doi.org/10.1021/bi0515873>.

- [22] T.J.T. Pinheiro, G.A. Elöve, A. Watts, H. Roder, Structural and kinetic description of cytochrome c unfolding induced by the interaction with lipid vesicles, *Biochemistry*. 36 (1997) 13122–13132, <https://doi.org/10.1021/bi971235z>.
- [23] J.B. Soffer, R. Schweitzer-Stenner, Near-exact enthalpy–entropy compensation governs the thermal unfolding of protonation states of oxidized cytochrome c, *J. Biol. Inorg. Chem.* 19 (2014) 1181–1194, <https://doi.org/10.1007/s00775-014-1174-x>.
- [24] L. Lancellotti, M. Borsari, M. Bellei, A. Bonifacio, C.A. Bortolotti, G. Di Rocco, A. Ranieri, M. Sola, G. Battistuzzi, Urea-induced denaturation of immobilized yeast iso-1 cytochrome c: role of Met80 and Tyr67 in the thermodynamics of unfolding and promotion of pseudoperoxidase and nitrite reductase activities, *Electrochim. Acta* 363 (2020), 137237, <https://doi.org/10.1016/j.electacta.2020.137237>.
- [25] A. Paradisi, L. Lancellotti, M. Borsari, M. Bellei, C.A. Bortolotti, G. Di Rocco, A. Ranieri, M. Sola, G. Battistuzzi, Met80 and Tyr67 affect the chemical unfolding of yeast cytochrome c: comparing the solution vs. immobilized state, *RSC, Chem. Biol.* 1 (2020) 421–435, <https://doi.org/10.1039/D0CB00115E>.
- [26] A. Guerra-Castellano, A. Díaz-Quintana, G. Pérez-Mejías, C.A. Elena-Real, K. González-Arzola, S.M. García-Mauriño, M.A. De la Rosa, I. Díaz-Moreno, Oxidative stress is tightly regulated by cytochrome c phosphorylation and respirasome factors in mitochondria, *Proc. Natl. Acad. Sci. U. S. A.* 115 (2018) 7955–7960, <https://doi.org/10.1073/pnas.1806833115>.
- [27] V.E. Kagan, H.A. Bayir, N.A. Belikova, O. Kapralov, Y.Y. Tyurina, V.A. Tyurin, J. Jiang, D.A. Stoyanovsky, P. Wipf, P.M. Kochanek, J.S. Greenberger, B. Pitt, A. A. Shvedova, G. Borisenko, Cytochrome c/Cardiolipin relations in mitochondria: a kiss of death, *Free Radic. Biol. Med.* 46 (2009) 1439–1453, <https://doi.org/10.1016/j.freeradbiomed.2009.03.004>.
- [28] B. Milorey, R. Schweitzer-Stenner, R. Kurbaj, D. Malyska, pH-induced switch between different modes of cytochrome c binding to Cardiolipin-containing liposomes, *ACS Omega* 4 (2019) 1386–1400, <https://doi.org/10.1021/acsomega.8b02574>.
- [29] P. Ascenzi, M. Coletta, M.T. Wilson, L. Fiorucci, M. Marino, F. Politicelli, F. Sinibaldi, R. Santucci, Cardiolipin-cytochrome c complex: switching cytochrome c from an electron-transfer shuttle to a myoglobin- and a peroxidase-like heme-protein, *IUBMB Life* 67 (2015) 98–109, <https://doi.org/10.1002/iub.1350>.
- [30] L. Fiorucci, F. Erba, R. Santucci, F. Sinibaldi, Cytochrome c interaction with Cardiolipin plays a key role in cell apoptosis: implications for human diseases, *Symmetry (Basel)*. 14 (2022) 767, <https://doi.org/10.3390/sym14040767>.
- [31] J. Martínez-Fábregas, I. Díaz-Moreno, K. González-Arzola, S. Janocha, J. A. Navarro, M. Hervás, R. Bernhardt, A. Velázquez-Campoy, A. Díaz-Quintana, M. A. De la Rosa, Structural and functional analysis of novel human cytochrome c targets in apoptosis, *Mol. Cell. Proteomics* 13 (2014) 1439–1456, <https://doi.org/10.1074/mcp.M113.034322>.
- [32] C.A. Fox, R.O. Ryan, Studies of the cardiolipin interactome, *Prog. Lipid Res.* 88 (2022), 101195, <https://doi.org/10.1016/j.plipres.2022.101195>.
- [33] A. Díaz-Quintana, G. Pérez-Mejías, A. Guerra-Castellano, M.A. De la Rosa, I. Díaz-Moreno, Wheel and Deal in the mitochondrial inner membranes: the tale of cytochrome c and Cardiolipin, *Oxidative Med. Cell. Longev.* 2020 (2020) 1–20, <https://doi.org/10.1155/2020/6813405>.
- [34] E. Kalanxhi, C.J.A.A. Wallace, Cytochrome c impaled: investigation of the extended lipid anchorage of a soluble protein to mitochondrial membrane models, *Biochem. J.* 407 (2007) 179–187, <https://doi.org/10.1042/BJ20070459>.
- [35] F. Sinibaldi, B.D. Howes, E. Droghetti, F. Politicelli, M.C. Piro, D. Di Pierro, L. Fiorucci, M. Coletta, G. Smulevich, R. Santucci, Role of Lysines in cytochrome c–Cardiolipin interaction, *Biochemistry*. 52 (2013) 4578–4588, <https://doi.org/10.1021/bi400324c>.
- [36] D. Mohammadyani, N. Yanamala, A.K. Samhan-Arias, A.A. Kapralov, G. Stepanov, N. Nuar, J. Planas-Iglesias, N. Sanghera, V.E. Kagan, J. Klein-Seetharaman, Structural characterization of cardiolipin-driven activation of cytochrome c into a peroxidase and membrane perturbation, *Biochim. Biophys. Acta Biomembr.* 2018 (1860) 1057–1068, <https://doi.org/10.1016/j.bbame.2018.01.009>.
- [37] L. Hannibal, F. Tomasina, D.A. Capdevila, V. Demicheli, V. Tórtora, D. Alvarez-Paggi, R. Jemmerson, D.H. Murgida, R. Radi, Alternative conformations of cytochrome c : structure, function, and detection, *Biochemistry*. 55 (2016) 407–428, <https://doi.org/10.1021/acs.biochem.5b01385>.
- [38] V.E. Kagan, A. Bayir, H. Bayir, D. Stoyanovsky, G.G. Borisenko, Y.Y. Tyurina, P. Wipf, J. Atkinson, J.S. Greenberger, R.S. Chapkin, N.A. Belikova, Mitochondria-targeted disruptors and inhibitors of cytochrome c/cardiolipin peroxidase complexes: a new strategy in anti-apoptotic drug discovery, *Mol. Nutr. Food Res.* 53 (2009) 104–114, <https://doi.org/10.1002/mnfr.200700402>.
- [39] A. Paradisi, M. Bellei, L. Paltrinieri, C.A. Bortolotti, G. Di Rocco, A. Ranieri, M. Borsari, M. Sola, G. Battistuzzi, Binding of S. Cerevisiae iso-1 cytochrome c and its surface lysine-to-alanine variants to cardiolipin: charge effects and the role of the lipid to protein ratio, *J. Biol. Inorg. Chem.* 25 (2020) 467–487, <https://doi.org/10.1007/s00775-020-01776-1>.
- [40] R.V. Chertkova, A.M. Firsov, N.A. Brazhe, E.I. Nikelshparg, Z.V. Bochkova, T. V. Bryantseva, M.A. Semenova, A.A. Baizhumanov, E.A. Kotova, M. P. Kirpichnikov, G.V. Maksimov, Y.N. Antonenko, D.A. Dolgikh, Multiple mutations in the non-ordered red Ω -loop enhance the membrane-Permeabilizing and peroxidase-like activity of cytochrome c, *Biomolecules*. 12 (2022) 1–15, <https://doi.org/10.3390/biom12050665>.
- [41] M. Li, W. Sun, V.A. Tyurin, M. DeLucia, J. Ahn, V.E. Kagan, P.C.A. van der Wel, Activation of cytochrome C peroxidase function through coordinated Foldon loop dynamics upon interaction with anionic lipids, *J. Mol. Biol.* 433 (2021), 167057, <https://doi.org/10.1016/j.jmb.2021.167057>.
- [42] M. Li, A. Mandal, V.A. Tyurin, M. DeLucia, J. Ahn, V.E. Kagan, P.C.A. van der Wel, Surface-binding to Cardiolipin Nanodomains triggers cytochrome c pro-apoptotic peroxidase activity via localized dynamics, *Structure*. (2019) 1–11, <https://doi.org/10.1016/j.str.2019.02.007>.
- [43] M. Abe, R. Niibayashi, S. Koubori, I. Moriyoama, H. Miyoshi, Molecular mechanisms for the induction of peroxidase activity of the cytochrome c-cardiolipin complex, *Biochemistry*. 50 (2011) 8383–8391, <https://doi.org/10.1021/bi2010202>.
- [44] R. Schweitzer-Stenner, Cytochrome c: a multifunctional protein combining conformational rigidity with flexibility, *New J. Sci.* 2014 (2014) 1–28, <https://doi.org/10.1155/2014/484538>.
- [45] J. Hanske, J.R. Toffey, A.M. Morenz, A.J. Bonilla, K.H. Schiavoni, E.V. Pletneva, Conformational properties of cardiolipin-bound cytochrome c, *Proc. Natl. Acad. Sci.* 109 (2012) 125–130, <https://doi.org/10.1073/pnas.1112312108>.
- [46] J. Muenzner, E.V. Pletneva, Structural transformations of cytochrome c upon interaction with cardiolipin, *Chem. Phys. Lipids* 179 (2014) 57–63, <https://doi.org/10.1016/j.chemphyslip.2013.11.002>.
- [47] L. Zeng, L. Wu, L. Liu, X. Jiang, Analyzing structural properties of heterogeneous cardiolipin-bound cytochrome c and their regulation by surface-enhanced infrared absorption spectroscopy, *Anal. Chem.* 88 (2016) 11727–11733, <https://doi.org/10.1021/acs.analchem.6b03360>.
- [48] L. Zeng, L. Wu, L. Liu, X. Jiang, The role of water distribution controlled by transmembrane potentials in the cytochrome c–Cardiolipin interaction: revealing from surface-enhanced infrared absorption spectroscopy, *Chem. - A Eur. J.* 23 (2017) 15491–15497, <https://doi.org/10.1002/chem.201703400>.
- [49] L. Milazzo, L. Tognaccini, B.D. Howes, F. Sinibaldi, M.C. Piro, M. Fittipaldi, M. C. Baratto, R. Pogni, R. Santucci, G. Smulevich, Unravelling the non-native low-spin state of the cytochrome c-Cardiolipin complex: evidence of the formation of a his-ligated species only, *Biochemistry*. 56 (2017) 1887–1898, <https://doi.org/10.1021/acs.biochem.6b01281>.
- [50] M.M. Elmer-Dixon, B.E. Bowler, Site A-mediated partial unfolding of cytochrome c on Cardiolipin vesicles is species-dependent and does not require Lys72, *Biochemistry*. 56 (2017) 4830–4839, <https://doi.org/10.1021/acs.biochem.7b00694>.
- [51] M.M. Elmer-Dixon, B.E. Bowler, Electrostatic constituents of the interaction of Cardiolipin with site a of cytochrome c, *Biochemistry*. 57 (2018) 5683–5695, <https://doi.org/10.1021/acs.biochem.8b00704>.
- [52] A. Thong, V. Tsoukanova, Cytochrome-c-assisted escape of cardiolipin from a model mitochondrial membrane, *Biochim. Biophys. Acta Biomembr.* 2018 (1860) 475–480, <https://doi.org/10.1016/j.bbame.2017.10.032>.
- [53] D.A. Capdevila, S. Oviedo Rouco, F. Tomasina, V. Tortora, V. Demicheli, R. Radi, D.H. Murgida, Active site structure and peroxidase activity of Oxidatively modified cytochrome c species in complexes with Cardiolipin, *Biochemistry*. 54 (2015) 7491–7504, <https://doi.org/10.1021/acs.biochem.5b00922>.
- [54] P.J.R. Spooner, A. Watts, Cytochrome c interactions with Cardiolipin in bilayers: a multinuclear magic-angle spinning NMR study, *Biochemistry*. 31 (1992) 10129–10138, <https://doi.org/10.1021/bi00156a037>.
- [55] L.V. Basova, I.V. Kurnikov, L. Wang, V.B. Ritov, N.A. Belikova, I.I. Vlasova, A. A. Pacheco, D.E. Winnica, J. Peterson, H. Bayir, D.H. Waldeck, V.E. Kagan, Cardiolipin switch in mitochondria: shutting off the reduction of cytochrome c and turning on the peroxidase activity, *Biochemistry*. 46 (2007) 3423–3434, <https://doi.org/10.1021/bi061854k>.
- [56] A.A. Kapralov, I.V. Kurnikov, I.I. Vlasova, N.A. Belikova, V.A. Tyurin, L. V. Basova, Q. Zhao, Y.Y. Tyurina, J. Jiang, H. Bayir, Y.A. Vladimirov, V.E. Kagan, The hierarchy of structural transitions induced in cytochrome c by anionic phospholipids determines its peroxidase activation and selective peroxidation during apoptosis in cells, *Biochemistry*. 46 (2007) 14232–14244, <https://doi.org/10.1021/bi701237b>.
- [57] F. Ripanti, A. Di Venere, M. Cestelli Guidi, M. Romani, A. Filabozzi, M. Carbonaro, M.C. Piro, F. Sinibaldi, A. Nucara, G. Mei, The puzzling problem of cardiolipin membrane-cytochrome c interactions: a combined infrared and fluorescence study, *Int. J. Mol. Sci.* 22 (2021) 1–15, <https://doi.org/10.3390/ijms22031334>.
- [58] H. Lei, A.D. Kelly, B.E. Bowler, Alkaline state of the domain-swapped dimer of human cytochrome c: a conformational switch for apoptotic peroxidase activity, *J. Am. Chem. Soc.* 144 (2022) 21184–21195, <https://doi.org/10.1021/jacs.2c08325>.
- [59] J. Zhan, G. Zhang, X. Chai, Q. Zhu, P. Sun, B. Jiang, X. Zhou, X. Zhang, M. Liu, Nmr reveals the conformational changes of cytochrome c upon interaction with cardiolipin, *Life*. 11 (2021) 1–12, <https://doi.org/10.3390/life11101031>.
- [60] J.A. Wilkinson, S. Silvera, P.J. LeBlanc, The effect of cardiolipin side chain composition on cytochrome c protein conformation and peroxidase activity, *Phys. Rep.* 9 (2021) 1–10, <https://doi.org/10.14814/phy2.14772>.
- [61] M.A. Proskurnin, E.V. Proskurnina, V.R. Galimova, A.V. Alekseev, I.V. Mikheev, Y.A. Vladimirov, Composition of the cytochrome c complex with Cardiolipin by thermal lens spectrometry, *Molecules*. 28 (2023) 1–16, <https://doi.org/10.3390/molecules28062692>.
- [62] S.C. Sun, H.W. Huang, Y.T. Lo, M.C. Chuang, Y.H.H. Hsu, Unraveling cardiolipin-induced conformational change of cytochrome c through H/D exchange mass spectrometry and quartz crystal microbalance, *Sci. Rep.* 11 (2021) 1–11, <https://doi.org/10.1038/s41598-020-79905-8>.
- [63] V. Demicheli, F. Tomasina, S. Sastre, A. Zeida, V. Tórtora, A. Lima, C. Batthyány, R. Radi, Cardiolipin interactions with cytochrome c increase tyrosine nitration

- yields and site-specificity, *Arch. Biochem. Biophys.* 703 (2021), <https://doi.org/10.1016/j.abb.2021.108824>.
- [64] F. Sinibaldi, L. Fiorucci, A. Patriarca, R. Lauceri, T. Ferri, M. Coletta, R. Santucci, Insights into cytochrome c-cardiolipin interaction. Role played by ionic strength, *Biochemistry*. 47 (2008) 6928–6935, <https://doi.org/10.1021/bi800048v>.
- [65] M.M. Elmer-Dixon, Z. Xie, J.B. Alverson, N.D. Priestley, B.E. Bowler, Curvature-dependent binding of cytochrome c to Cardiolipin, *J. Am. Chem. Soc.* 142 (2020) 19532–19539, <https://doi.org/10.1021/jacs.0c07301>.
- [66] C. Fu, Y. Sun, C. Huang, F. Wang, N. Li, L. Zhang, S. Ge, J. Yu, Ultrasensitive sandwich-like electrochemical biosensor based on core-shell Pt@CeO₂ as signal tags and double molecular recognition for cerebral dopamine detection, *Talanta*. 223 (2021), 121719, <https://doi.org/10.1016/j.talanta.2020.121719>.
- [67] Y. Hong, J. Muenzner, S.K. Grimm, E.V. Pletneva, Origin of the conformational heterogeneity of cardiolipin-bound cytochrome c, *J. Am. Chem. Soc.* 134 (2012) 18713–18723, <https://doi.org/10.1021/ja307426k>.
- [68] J. Planas-Iglesias, H. Dwarakanath, D. Mohamadyani, N. Yanamala, V.E. Kagan, J. Klein-Seetharaman, Cardiolipin interactions with proteins, *Biophys. J.* 109 (2015) 1282–1294, <https://doi.org/10.1016/j.bpj.2015.07.034>.
- [69] F. Sinibaldi, L. Milazzo, B.D. Howes, M.C. Piro, L. Fiorucci, F. Polticelli, P. Ascenzi, M. Coletta, G. Smulevich, R. Santucci, The key role played by charge in the interaction of cytochrome c with cardiolipin, *JBIC J. Biol. Inorg. Chem.* 22 (2017) 19–29, <https://doi.org/10.1007/s00775-016-1404-5>.
- [70] E.K.J. Tuominen, C.J.A. Wallace, P.K.J. Kinnunen, Phospholipid-cytochrome c interaction. Evidence for the extended lipid anchorage, *J. Biol. Chem.* 277 (2002) 8822–8826, <https://doi.org/10.1074/jbc.M200056200>.
- [71] M. Rytömaa, P.K.J. Kinnunen, Reversibility of the binding of cytochrome c to liposomes. Implications for lipid-protein interactions, *J. Biol. Chem.* 270 (1995) 3197–3202, <https://doi.org/10.1074/jbc.270.7.3197>.
- [72] M. Rytömaa, P.K.J. Kinnunen, Evidence for two distinct acidic phospholipid-binding sites in cytochrome c, *J. Biol. Chem.* 269 (1994) 1770–1774.
- [73] F. Sinibaldi, B.D. Howes, M.C. Piro, F. Polticelli, C. Bombelli, T. Ferri, M. Coletta, G. Smulevich, R. Santucci, Extended cardiolipin anchorage to cytochrome c: a model for protein-mitochondrial membrane binding, *J. Biol. Inorg. Chem.* 15 (2010) 689–700, <https://doi.org/10.1007/s00775-010-0636-z>.
- [74] B.S. Rajagopal, G.G. Silkstone, P. Nicholls, M.T. Wilson, J.A.R. Worrall, An investigation into a cardiolipin acyl chain insertion site in cytochrome c, *Biochim. Biophys. Acta Bioenerg.* 2012 (1817) 780–791, <https://doi.org/10.1016/j.bbabi.2012.02.010>.
- [75] F. Sinibaldi, E. Droghetti, F. Polticelli, M.C. Piro, D. Di Pierro, T. Ferri, G. Smulevich, R. Santucci, The effects of ATP and sodium chloride on the cytochrome c-cardiolipin interaction: the contrasting behavior of the horse heart and yeast proteins, *J. Inorg. Biochem.* 105 (2011) 1365–1372, <https://doi.org/10.1016/j.jinorgbio.2011.07.022>.
- [76] J. Muenzner, J.R. Toffey, Y. Hong, E.V. Pletneva, Becoming a peroxidase: Cardiolipin-induced unfolding of cytochrome c, *J. Phys. Chem. B* 117 (2013) 12878–12886, <https://doi.org/10.1021/jp402104r>.
- [77] E.J. Snider, J. Muenzner, J.R. Toffey, Y. Hong, E.V. Pletneva, Multifaceted effects of ATP on Cardiolipin-bound cytochrome c, *Biochemistry*. 52 (2013) 993–995, <https://doi.org/10.1021/bi301682c>.
- [78] C. Nunez, J.J. Trivino, V. Arancibia, A electrochemical biosensor for as(III) detection based on the catalytic activity of Alcaligenes faecalis immobilized on a gold nanoparticle-modified screen-printed carbon electrode, *Talanta*. 223 (2021), 121702, <https://doi.org/10.1016/j.talanta.2020.121702>.
- [79] L.A. Pandiscia, R. Schweitzer-Stenner, Coexistence of native-like and non-native cytochrome c on anionic liposomes with different Cardiolipin content, *J. Phys. Chem. B* 119 (2015) 12846–12859, <https://doi.org/10.1021/acs.jpcc.5b07328>.
- [80] J.M. Bradley, G. Silkstone, M.T. Wilson, M.R. Cheesman, J.N. Butt, Probing a complex of cytochrome c and cardiolipin by magnetic circular dichroism spectroscopy: implications for the initial events in apoptosis, *J. Am. Chem. Soc.* 133 (2011) 19676–19679, <https://doi.org/10.1021/ja209144h>.
- [81] A. Ranieri, D. Millo, G. Di Rocco, G. Battistuzzi, C.A. Bortolotti, M. Borsari, M. Sola, Immobilized cytochrome c bound to cardiolipin exhibits peculiar oxidation state-dependent axial heme ligation and catalytically reduces dioxygen, *JBIC J. Biol. Inorg. Chem.* 20 (2015) 531–540, <https://doi.org/10.1007/s00775-015-1238-6>.
- [82] A. Ranieri, G. Di Rocco, D. Millo, G. Battistuzzi, C.A. Bortolotti, L. Lancellotti, M. Borsari, M. Sola, Thermodynamics and kinetics of reduction and species conversion at a hydrophobic surface for mitochondrial cytochromes c and their cardiolipin adducts, *Electrochim. Acta* 176 (2015) 1019–1028, <https://doi.org/10.1016/j.electacta.2015.07.065>.
- [83] G. Di Rocco, B. Bigli, M. Borsari, C.A. Bortolotti, A. Ranieri, M. Sola, G. Battistuzzi, Electron transfer and electrocatalytic properties of the immobilized Met80Ala cytochrome c variant in Dimethylsulfoxide, *ChemElectroChem*. 8 (2021) 2115–2123, <https://doi.org/10.1002/celec.202100499>.
- [84] L.C. Godoy, C. Muñoz-Pinedo, L. Castro, S. Cardaci, C.M. Schonhoff, M. King, V. Tórtora, M. Marín, Q. Miao, J.F. Jiang, A. Kapralov, R. Jemerson, G. Silkstone, J.N. Patel, J.E. Evans, M.T. Wilson, D.R. Green, V.E. Kagan, R. Radi, J.B. Mannick, Disruption of the M80-Fe ligation stimulates the translocation of cytochrome c to the cytoplasm and nucleus in nonapoptotic cells, *Proc. Natl. Acad. Sci.* 106 (2009) 2653–2658, <https://doi.org/10.1073/pnas.0809279106>.
- [85] S. Casalini, G. Battistuzzi, M. Borsari, C.A. Bortolotti, A. Ranieri, M. Sola, Electron transfer and electrocatalytic properties of the immobilized Methionine80Alanine cytochrome c variant, *J. Phys. Chem. B* 112 (2008) 1555–1563, <https://doi.org/10.1021/jp0765953>.
- [86] S. Casalini, G. Battistuzzi, M. Borsari, A. Ranieri, M. Sola, Catalytic reduction of dioxygen and nitrite ion at a Met80Ala cytochrome c-functionalized electrode, *J. Am. Chem. Soc.* 130 (2008) 15099–15104, <https://doi.org/10.1021/ja8040724>.
- [87] S. Casalini, G. Battistuzzi, M. Borsari, C.A. Bortolotti, G. Di Rocco, A. Ranieri, M. Sola, Electron transfer properties and hydrogen peroxide electrocatalysis of cytochrome c variants at positions 67 and 80, *J. Phys. Chem. B* 114 (2010) 1698–1706, <https://doi.org/10.1021/jp9090365>.
- [88] A. Ranieri, G. Battistuzzi, M. Borsari, C.A. Bortolotti, G. Di Rocco, S. Monari, M. Sola, A bis-histidine-ligated unfolded cytochrome c immobilized on anionic SAM shows pseudo-peroxidase activity, *Electrochem. Commun.* 14 (2012) 29–31, <https://doi.org/10.1016/j.elecom.2011.10.021>.
- [89] A. Ranieri, C.A. Bortolotti, G. Battistuzzi, M. Borsari, L. Paltrinieri, G. Di Rocco, M. Sola, Effect of motional restriction on the unfolding properties of a cytochrome c featuring a his/met-his ligation switch, *Metallomics*. 6 (2014) 874, <https://doi.org/10.1039/c3mt00311f>.
- [90] A. Ranieri, M. Borsari, S. Casalini, G. Di Rocco, M. Sola, C.A. Bortolotti, G. Battistuzzi, How to turn an Electron transfer protein into a redox enzyme for biosensing, *Molecules*. 26 (2021) 4950, <https://doi.org/10.3390/molecules26164950>.
- [91] A.A. Kapralov, N. Yanamala, Y.Y. Tyurina, L. Castro, A. Samhan-Arias, Y. A. Vladimirov, A. Maeda, A.A. Weitz, J. Peterson, D. Mylnikov, V. Demicheli, V. Tortora, J. Klein-Seetharaman, R. Radi, V.E. Kagan, Topography of tyrosine residues and their involvement in peroxidation of polyunsaturated cardiolipin in cytochrome c/cardiolipin peroxidase complexes, *Biochim. Biophys. Acta Biomembr.* 2011 (1808) 2147–2155, <https://doi.org/10.1016/j.bbame.2011.04.009>.
- [92] J.M. García-Heredia, I. Díaz-Moreno, P.M. Nieto, M. Orzáez, S. Kocanis, M. Teixeira, E. Pérez-Payá, A. Díaz-Quintana, M.A. De la Rosa, Nitration of tyrosine 74 prevents human cytochrome c to play a key role in apoptosis signaling by blocking caspase-9 activation, *Biochim. Biophys. Acta Bioenerg.* 1797 (2010) 981–993, <https://doi.org/10.1016/j.bbabi.2010.03.009>.
- [93] I. Díaz-Moreno, J.M. García-Heredia, A. Díaz-Quintana, M. Teixeira, M.A. De la Rosa, Nitration of tyrosines 46 and 48 induces the specific degradation of cytochrome c upon change of the heme iron state to high-spin, *Biochim. Biophys. Acta Bioenerg.* 2011 (1807) 1616–1623, <https://doi.org/10.1016/j.bbabi.2011.09.012>.
- [94] J.M. García-Heredia, A. Díaz-Quintana, M. Salzano, M. Orzáez, E. Pérez-Payá, M. Teixeira, M.A. De la Rosa, I. Díaz-Moreno, Tyrosine phosphorylation turns alkaline transition into a biologically relevant process and makes human cytochrome c behave as an anti-apoptotic switch, *JBIC J. Biol. Inorg. Chem.* 16 (2011) 1155–1168, <https://doi.org/10.1007/s00775-011-0804-9>.
- [95] G. Di Rocco, A. Ranieri, C.A. Bortolotti, G. Battistuzzi, A. Bonifacio, V. Sergio, M. Borsari, M. Sola, Axial iron coordination and spin state change in a heme c upon electrostatic protein-SAM interaction, *Phys. Chem. Chem. Phys.* 15 (2013) 13499, <https://doi.org/10.1039/c3cp50222h>.
- [96] Y. Lu, D.R. Casimiro, K.L. Bren, J.H. Richards, H.B. Gray, Structurally engineered cytochromes with unusual ligand-binding properties: expression of Saccharomyces cerevisiae Met-80 → ala iso-1-cytochrome c, *Proc. Natl. Acad. Sci.* 90 (1993) 11456–11459, <https://doi.org/10.1073/pnas.90.24.11456>.
- [97] K.L. Bren, H.B. Gray, Structurally engineered cytochromes with novel ligand-binding sites: oxy and carbon monoxide derivatives of semisynthetic horse heart Ala80 cytochrome c, *J. Am. Chem. Soc.* 115 (1993) 10382–10383, <https://doi.org/10.1021/ja00075a073>.
- [98] G. Di Rocco, G. Battistuzzi, A. Ranieri, C.A. Bortolotti, M. Borsari, M. Sola, Thermodynamics and kinetics of Electron transfer of electrode-immobilized small laccase from Streptomyces coelicolor, *Molecules*. 27 (2022) 8079, <https://doi.org/10.3390/molecules27228079>.
- [99] G. Battistuzzi, C.A. Bortolotti, M. Bellei, G. Di Rocco, J. Salewski, P. Hildebrandt, M. Sola, Role of Met80 and Tyr67 in the low-pH conformational equilibria of cytochrome c, *Biochemistry*. 51 (2012) 5967–5978, <https://doi.org/10.1021/bi3007302>.
- [100] L. Banci, I. Bertini, K.L. Bren, H.B. Gray, P. Turano, pH-dependent equilibria of yeast Met80Ala-iso-1-cytochrome c probed by NMR spectroscopy: a comparison with the wild-type protein, *Chem. Biol.* 2 (1995) 377–383, [https://doi.org/10.1016/1074-5521\(95\)90218-X](https://doi.org/10.1016/1074-5521(95)90218-X).
- [101] K.L. Bren, H.B. Gray, L. Banci, I. Bertini, P. Turano, Paramagnetic 1H NMR spectroscopy of the cyanide derivative of Met80Ala-iso-1-cytochrome c, *J. Am. Chem. Soc.* 117 (1995) 8067–8073, <https://doi.org/10.1021/ja00136a003>.
- [102] M. Patriarca, T. Eliseo, F. Sinibaldi, M.C. Piro, R. Melis, M. Paci, D.O. Cicero, F. Polticelli, R. Santucci, L. Fiorucci, ATP acts as a regulatory effector in modulating structural transitions of cytochrome c: implications for apoptotic activity, *Biochemistry*. 48 (2009) 3279–3287, <https://doi.org/10.1021/bi801837e>.
- [103] C.A. Bortolotti, G. Battistuzzi, M. Borsari, P. Facci, A. Ranieri, M. Sola, The redox chemistry of the covalently immobilized native and low-pH forms of yeast Iso-1-cytochrome c, *J. Am. Chem. Soc.* 128 (2006) 5444–5451, <https://doi.org/10.1021/ja0573662>.
- [104] M. Fedurco, J. Augustynski, C. Indiani, G. Smulevich, M. Antalík, M. Bánó, E. Sedláčková, M.C. Glascock, J.H. Dawson, The heme iron coordination of unfolded ferric and ferrous cytochrome c in neutral and acidic urea solutions. Spectroscopic and electrochemical studies, *Biochim. Biophys. Acta - Proteins, Proteomics*. 1703 (2004) 31–41, <https://doi.org/10.1016/j.bbapap.2004.09.013>.
- [105] A.M. Berghuis, J.G. Guillemette, M. Smith, G.D. Brayer, Mutation of tyrosine-67 to phenylalanine in cytochrome c significantly alters the local heme environment, *J. Mol. Biol.* 235 (1994) 1326–1341, <https://doi.org/10.1006/jmbi.1994.1086>.

- [106] F. Paulat, N. Lehnert, Detailed assignment of the magnetic circular dichroism and UV–Vis spectra of five-coordinate high-spin ferric [Fe(TPP)(Cl)], *Inorg. Chem.* 47 (2008) 4963–4976, <https://doi.org/10.1021/ic8002838>.
- [107] M. Bellei, C.A. Bortolotti, G. Di Rocco, M. Borsari, L. Lancellotti, A. Ranieri, M. Sola, G. Battistuzzi, The influence of the Cys46/Cys55 disulfide bond on the redox and spectroscopic properties of human neuroglobin, *J. Inorg. Biochem.* 178 (2018) 70–86, <https://doi.org/10.1016/j.jinorgbio.2017.10.005>.
- [108] G. Di Rocco, G. Battistuzzi, C.A. Bortolotti, M. Borsari, E. Ferrari, S. Monari, M. Sola, Cloning, expression, and physicochemical characterization of a new diheme cytochrome c from *Shewanella baltica* OS155, *JBIC J. Biol. Inorg. Chem.* 16 (2011) 461–471, <https://doi.org/10.1007/s00775-010-0742-y>.
- [109] L.A. Pandiscia, R. Schweitzer-Stenner, Coexistence of native-like and non-native partially unfolded Ferricytochrome c on the surface of Cardiolipin-containing liposomes, *J. Phys. Chem. B* 119 (2015) 1334–1349, <https://doi.org/10.1021/jp5104752>.
- [110] G. Di Rocco, A. Ranieri, M. Borsari, M. Sola, C.A. Bortolotti, G. Battistuzzi, Assessing the functional and structural stability of the Met80Ala mutant of cytochrome c in Dimethylsulfoxide, *Molecules* 27 (2022), <https://doi.org/10.3390/molecules27175630>.
- [111] L. Banci, I. Bertini, K.L. Bren, H.B. Gray, P. Somponpisut, P. Turano, Three-dimensional solution structure of the cyanide adduct of a variant of *Saccharomyces cerevisiae* Iso-1-cytochrome c containing the Met80Ala mutation. Identification of Ligand-Residue Interactions in the Distal Heme Cavity, *Biochemistry* 34 (1995) 11385–11398, <https://doi.org/10.1021/bi00036a011>.
- [112] L.A. Pandiscia, R. Schweitzer-Stenner, Salt as a catalyst in the mitochondria: returning cytochrome c to its native state after it misfolds on the surface of cardiolipin containing membranes, *Chem. Commun.* 50 (2014) 3674–3676, <https://doi.org/10.1039/c3cc48709a>.
- [113] A.M. Davies, J.G. Guillemette, M. Smith, C. Greenwood, A.G.P. Thurgood, A. G. Mauk, G.R. Moore, Redesign of the interior hydrophilic region of mitochondrial cytochrome c by site-directed mutagenesis, *Biochemistry* 32 (1993) 5431–5435, <https://doi.org/10.1021/bi00071a019>.
- [114] H.R. Schroeder, F.A. McOdimba, J.G. Guillemette, J.A. Kornblatt, The polarity of tyrosine 67 in yeast iso-1-cytochrome c monitored by second derivative spectroscopy, *Biochem. Cell Biol.* 75 (1997) 191–197.
- [115] N. Sanghera, T.J.T. Pinheiro, Unfolding and refolding of cytochrome c driven by the interaction with lipid micelles, *Protein Sci.* 9 (2009) 1194–1202, <https://doi.org/10.1110/ps.9.6.1194>.
- [116] D.W. Urry, The heme chromophore in the ultraviolet, *J. Biol. Chem.* 242 (1967) 4441–4448.
- [117] E.H. Strickland, S. Beychok, Aromatic contributions to circular dichroism spectra of protein, *CRC Crit. Rev. Biochem.* 2 (1974) 113–175, <https://doi.org/10.3109/10409237409105445>.
- [118] L. Serpas, B. Milorey, L.A. Pandiscia, A.W. Addison, R. Schweitzer-Stenner, Autoxidation of reduced horse heart cytochrome c catalyzed by Cardiolipin-containing membranes, *J. Phys. Chem. B* 120 (2016) 12219–12231, <https://doi.org/10.1021/acs.jpcc.6b05620>.
- [119] A.E. Pond, M. Sono, E.A. Elenkova, D.B. Goodin, A.M. English, J.H. Dawson, Influence of protein environment on magnetic circular dichroism spectral properties of ferric and ferrous ligand complexes of yeast cytochrome c peroxidase, *Biospectroscopy* 5 (1999) 42–52, [https://doi.org/10.1002/\(sici\)1520-6343\(1999\)5:5+<s42::aid-bsp5>3.0.co;2-9](https://doi.org/10.1002/(sici)1520-6343(1999)5:5+<s42::aid-bsp5>3.0.co;2-9).
- [120] F. Neri, D. Kok, M.A. Miller, G. Smulevich, Fluoride binding in hemoproteins: the importance of the distal cavity structure, *Biochemistry* 36 (1997) 8947–8953.
- [121] G. Battistuzzi, M. Bellei, C.A. Bortolotti, G. Di Rocco, A. Leonardi, M. Sola, Characterization of the solution reactivity of a basic heme peroxidase from *Cucumis sativus*, *Arch. Biochem. Biophys.* 423 (2004) 317–331, <https://doi.org/10.1016/j.abb.2003.12.036>.
- [122] B. Milorey, D. Malyska, R. Schweitzer-Stenner, pH dependence of Ferricytochrome c conformational transitions during binding to Cardiolipin membranes: evidence for histidine as the distal ligand at neutral pH, *J. Phys. Chem. Lett.* 8 (2017) 1993–1998, <https://doi.org/10.1021/acs.jpclett.7b00597>.
- [123] J.S. Milne, Y. Xu, L.C. Mayne, S.W. Englander, Experimental study of the protein folding landscape: unfolding reactions in cytochrome c, *J. Mol. Biol.* 290 (1999) 811–822, <https://doi.org/10.1006/jmbi.1999.2924>.
- [124] L. Hoang, S. Bédard, M.M.G. Krishna, Y. Lin, S.W. Englander, Cytochrome c folding pathway: kinetic native-state hydrogen exchange, *Proc. Natl. Acad. Sci. U. S. A.* 99 (2002) 12173–12178, <https://doi.org/10.1073/pnas.152439199>.
- [125] L. Hoang, H. Maity, M.M.G. Krishna, Y. Lin, S.W. Englander, Folding units govern the cytochrome c alkaline transition, *J. Mol. Biol.* 331 (2003) 37–43, [https://doi.org/10.1016/S0022-2836\(03\)00698-3](https://doi.org/10.1016/S0022-2836(03)00698-3).
- [126] H. Maity, M. Maity, M.M.G. Krishna, L. Mayne, S.W. Englander, Protein folding: the stepwise assembly of foldon units, *Proc. Natl. Acad. Sci.* 102 (2005) 4741–4746, <https://doi.org/10.1073/pnas.0501043102>.
- [127] G. Battistuzzi, M. Borsari, J.A. Cowan, A. Ranieri, M. Sola, Control of cytochrome c redox potential: axial ligation and protein environment effects, *J. Am. Chem. Soc.* 124 (2002) 5315–5324, <https://doi.org/10.1021/ja017479v>.
- [128] G. Balakrishnan, Y. Hu, T.G. Spiro, R.A. Copeland, T.G. Spiro, G. Balakrishnan, Y. Hu, T.G. Spiro, His26 protonation in cytochrome c triggers microsecond β -sheet formation and heme exposure: implications for apoptosis, *J. Am. Chem. Soc.* 134 (2012) 19061–19069, <https://doi.org/10.1021/ja307100a>.
- [129] F. Sinibaldi, M.C. Piro, B.D. Howes, G. Smulevich, F. Ascoli, R. Santucci, Rupture of the hydrogen bond linking two ω -loops induces the molten globule state at neutral pH in cytochrome c, *Biochemistry* 42 (2003) 7604–7610, <https://doi.org/10.1021/bi034132r>.
- [130] R. Schweitzer-Stenner, Heme–protein interactions and functional relevant heme deformations: the cytochrome c case, *Molecules* 27 (2022), <https://doi.org/10.3390/molecules27248751>.
- [131] I. Dragomir, A. Hagarman, C. Wallace, R. Schweitzer-Stenner, Optical band splitting and electronic perturbations of the heme chromophore in cytochrome c at room temperature probed by visible electronic circular dichroism spectroscopy, *Biophys. J.* 92 (2007) 989–998, <https://doi.org/10.1529/biophysj.106.095976>.